

ANALYSIS OF SEMICONDUCTOR LASER DIODES FOR
HIGH BIT-RATE VISIBLE LIGHT COMMUNICATION

BY

MD HOSNE MOBAROK SHAMIM

A Thesis Presented to the
DEANSHIP OF GRADUATE STUDIES

KING FAHD UNIVERSITY OF PETROLEUM & MINERALS

DHAHRAN, SAUDI ARABIA

In Partial Fulfillment of the
Requirements for the Degree of

MASTER OF SCIENCE

In

ELECTRICAL ENGINEERING

APRIL, 2018

KING FAHD UNIVERSITY OF PETROLEUM & MINERALS

DHAHRAN- 31261, SAUDI ARABIA

DEANSHIP OF GRADUATE STUDIES

This thesis, written by **MD HOSNE MOBAROK SHAMIM** under the direction of his thesis advisor and approved by his thesis committee, has been presented and accepted by the Dean of Graduate Studies, in partial fulfillment of the requirements for the degree of **MASTER OF SCIENCE IN ELECTRICAL ENGINEERING**.

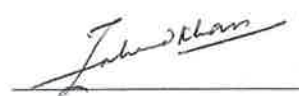


Dr. Ali Ahmad Al-Shaikhi
Department Chairman



Dr. Salam A. Zummo
Dean of Graduate Studies

02/07/2018
Date



Dr. Mohammed Zahed Mustafa
Khan
(Advisor)



Dr. Samir Al-Ghadhban
(Member)



Dr. Khurram Karim Qureshi
(Member)

© Md Hosne Mobarok Shamim

2018

Dedicated to

My parents, Md. Mohshin Ali and Nazera Khanam,

My wife, Khadija Bint Abdur Rouf, and

My sisters, Jannatul Ferdous and Ismat Ara Ferdous

for your continuous support and inspiration

ACKNOWLEDGMENTS

All praises to Allah, who made my journey to pursue higher studies easy, enjoyable, and successful. My sincere thanks to the government of Saudi Arabia to provide me with a generous scholarship and giving me the chance to be a part of King Fahd University of Petroleum & Minerals as a graduate student.

It was an outstanding journey especially because of my supervisor Dr. Mohammed Zahed Mustafa Khan, who was always there whenever I needed support. I have learned a lot from him which will surely help me become an accomplished researcher and good human being in the future. He used to say that master's degree is training for a Ph.D. degree and eventually for a career in research and academia. I must say that he trained me well.

I would like to thank my committee members: Dr. Samir Alghadhban and Dr. Khurram Karim Qureshi for their useful responses, advice and the time they have spent reviewing this thesis. I have found their company quite encouraging which I believe is very important for a graduate student.

It was my immense pleasure to spend almost a year at the Photonics Laboratory of King Abdullah University of Science and Technology (KAUST), Thuwal, Saudi Arabia. I am grateful to Professor Boon S. Ooi and Dr. Tien Khee Ng for their guidance, suggestions, and encouragement. I will always remember the meetings with Prof. Ooi and Dr. Tien Khee which helped me shape my future goal. All the lab members were very accommodating and friendly, a big thanks to you all. Among the lab members, I must mention few if not all; Dr. Chao Shen, Dr. Hassan Oubei were great mentors who taught me photonics from

the very basics. My collaborator, Dr. Yuan Mao, Xiaobin Sun, Wenqi Cai, and Omar Alkhazragi, a big thanks to you too. It was such an experience at the Photonics Lab, which I will cherish forever. I am so grateful to the people of KAUST for arranging everything that I needed and responding promptly to my every problem.

Finally, I am blessed to be the son of great parents, husband of a loving and caring wife, and brother of the most encouraging sisters. It is them who has continuously motivated me to take every challenge in my life. It wouldn't have been possible without their support. Thank you.

TABLE OF CONTENTS

ACKNOWLEDGMENTS	V
TABLE OF CONTENTS	VII
LIST OF TABLES	X
LIST OF FIGURES	XI
LIST OF ABBREVIATION	XIV
ABSTRACT	XVII
ملخص الرسالة	XIX
CHAPTER 1 INTRODUCTION	1
1.1 Visible light communication	2
1.1.1 Transmitter	4
1.1.2 Receiver	5
1.2 Injection locking	6
1.2.1 External injection locking (EIL)	6
1.2.2 Self-injection locking (SIL)	7
1.3 Research motivation	7
1.4 Research objectives	8
1.5 Research methodology	9
CHAPTER 2 DEVICE CHARACTERIZATION	12
2.1 450 nm blue laser diode	13
2.1.1 LIV characteristics	13
2.1.2 Lasing emission spectrum	16

2.1.3 Small signal modulation response	17
2.2 520 nm green laser diode	18
2.2.1 LIV characteristics	18
2.2.2 Lasing emission spectrum	20
2.2.3 Small signal modulation response	20
2.3 638 nm red laser diode	21
2.3.1 LIV characteristics	21
2.3.2 Lasing emission spectrum	23
2.3.3 Small signal modulation response	23
CHAPTER 3 SELF-INJECTION LOCKING CHARACTERIZATION	25
3.1 Self-injection locking experimental setup	28
3.2 LIV characteristics of Self-injection locked laser diodes	30
3.3 Emission spectrum of Self-injection locked laser diode	32
3.4 Small signal modulation of Self-injection locked laser diode	35
3.5 Stability of the Self-injection locking	38
3.6 Effect of injection current on Self-injection locking	39
3.7 Effect of injection ratio on Self-injection locking	45
3.8 Effect of external cavity length on Self-injection locking	51
CHAPTER 4 VISIBLE LIGHT COMMUNICATION	54
4.1 On-off keying (OOK)	54
4.1.1 Effect of the NRZ modulating signal on the SNR:	55
4.1.2 Effect of the NRZ modulating signal on the peak wavelengths:	57
4.1.3 Communication using blue laser diode:	57
4.1.4 Communication using green laser diode:	61

4.1.5 Communication using red laser diode:	64
4.2 Performance analysis of the self-injection locked laser using OOK.....	66
CHAPTER 5 CONCLUSION.....	68
5.1 Summary of the research contribution	68
5.2 Future work	69
REFERENCES.....	70
VITAE.....	74

LIST OF TABLES

Table 1-1	Elements of a visible light communication link	4
Table 2-1	Laser diode parameters obtained from the manufacturer [12]–[14]	12
Table 3-1	Performance comparison of 26 and 56 cm external cavity lengths on self-injection locked BGR laser diodes	52
Table 4-1	Eye diagram of the VLC with 450 nm laser diode as a transmitter	59
Table 4-2	Eye diagram for various data rate are compared between free running and locked 520 nm green laser diodes	62
Table 4-3	Eye diagram for various data rate are compared between free running and locked 638 nm red laser diodes	65

LIST OF FIGURES

Figure 1-1	Visible portion of the electromagnetic spectrum. The ranges are marked in nanometer wavelength	2
Figure 1-2	Basic Elements in Visible Light Communication system.....	3
Figure 1-3	Basic structure of a homojunction laser diode (left) and a sample of commercially available TO can laser diode (right)	5
Figure 1-4	External injection locking block diagram	6
Figure 1-5	Self-injection locking block diagram	7
Figure 1-8	Block diagram of a free space self-injection locking setup	10
Figure 1-9	Laboratory photograph of the self injection locking setup.....	11
Figure 2-1	Safety enclosure for the experimental setup	13
Figure 2-2	L-I characteristics of 450 nm blue TO can laser diode	15
Figure 2-3	V-I characteristics of the 450 nm blue TO can laser diode.....	15
Figure 2-4	Emission spectrum of 450 nm blue laser diode at various injection currents.....	16
Figure 2-5	Small signal modulation of 450 nm blue laser diode	18
Figure 2-6	L-I characteristics of 520 nm green laser diode	19
Figure 2-7	V-I characteristics of 520 nm green laser diode.....	19
Figure 2-8	Emission spectrum of 520 nm green laser diode at various injection currents.....	20
Figure 2-9	Small signal modulation of 520 nm green laser diode at various injection current	21
Figure 2-10	L-I curve for 638 nm, red laser diode	22
Figure 2-11	V-I curve of the 638 nm red laser diode	22
Figure 2-12	Emission spectrum of 638 nm red laser diode	23
Figure 2-13	Small signal modulation of 638 nm red laser diode.....	24
Figure 3-1	(a) Schematic of the self-injection locking experimental setup. (b) Laboratory photograph of the experimental setup	29
Figure 3-2	Comparison of the optical power and voltage characteristics of blue laser diode versus injection current, under the free running and self-injection locked cases.	31
Figure 3-3	Comparison of the optical power and voltage characteristics of green laser diode versus injection current, under the free running and self-injection locked cases.	31
Figure 3-4	Comparison of the optical power and voltage characteristics of red laser diode versus injection current, under the free running and self-injection locked cases.	32
Figure 3-5	The lasing spectrum under self-injected locked and free running case for blue laser diodes.....	34

Figure 3-6	The lasing spectrum under self-injected locked and free running case for green laser diodes.....	34
Figure 3-7	The lasing spectrum under self-injected locked and free running case for red laser diodes.	35
Figure 3-8	The small signal modulation response of 450 nm laser diode in free running and the injection locked case.....	36
Figure 3-9	Frequency response of 520 nm green laser diode comparing the response of a solitary laser with the self injection locked laser.....	37
Figure 3-10	The small signal modulation response of 638 nm red laser diode for the free running and the injection locked case.....	37
Figure 3-11	Short-term stability analysis of (a) and (d) blue, (b) and (e) green, and (c) and (f) red self-injection locked laser diodes.....	39
Figure 3-12	Variation of the modulation bandwidth as a function of injection current for blue laser diodes.	41
Figure 3-13	Variation of the modulation bandwidth as a function of injection current for green laser diodes.....	41
Figure 3-14	Variation of the modulation bandwidth as a function of injection current for red laser diodes.....	42
Figure 3-15	Variation of the spectral linewidth as a function of injection current for blue laser diodes.....	44
Figure 3-16	Variation of the spectral linewidth as a function of injection current for green laser diodes.....	44
Figure 3-17	Variation of the Spectral linewidth as a function of injection current for red laser diodes.	45
Figure 3-18	Variation of the modulation bandwidth as a function of injection ratio for the blue laser diode.	47
Figure 3-19	Variation of the modulation bandwidth as a function of injection ratio for the green laser diode.	47
Figure 3-20	Variation of the modulation bandwidth as a function of injection ratio for the red laser diode.	48
Figure 3-21	Variation of the spectral linewidth as a function of injection ratio for the blue laser diode.	50
Figure 3-22	Variation of the spectral linewidth as a function of injection ratio for the green laser diode.	50
Figure 3-23	Variation of the spectral linewidth as a function of injection ratio for the red laser diode.....	51
Figure 3-24	Variation of the spectral linewidth (top row) and modulation bandwidth (bottom row) as a function of injection current for blue (a) and (d), green (b) and (e), and red (c) and (f) laser diodes.	53
Figure 4-1	Block diagram of On Off Keying (OOK) setup.....	55

Figure 4-2	Performance of VLC using a 638 nm red LD at various amplitude of the NRZ modulating signal.....	56
Figure 4-3	Peak wavelength shift of the free running and locked laser at variable amplitude of the modulating signal	57
Figure 4-4	Optical spectrum comparing the free running and locked spectrum at 78 mA injection current	58
Figure 4-5	Bit error rate of free running (black) and locked (blue) laser at various data rate.....	61
Figure 4-6	Calculated BER for free running and locked 520 nm green laser diode in OOK modulation scheme.....	64
Figure 4-7	Bit error rate (BER) for free running and locked 638 nm red laser diode in OOK modulation scheme.	66

LIST OF ABBREVIATION

VLC	:	Visible Light Communication
RF	:	Radio Frequency
LD	:	Laser Diode
LASER	:	Light Amplification by Stimulated Emission of Radiation
BGR	:	Bragg Grating Reflector
DFB	:	Distributed Feedback
LED	:	Light Emitting Diode
APD	:	Avalanche Photo Detector
TO can	:	Top Open can
OCW	:	Optical Wireless Communication
Li-Fi	:	Light Fidelity
NIR	:	Near Infrared
Tx	:	Transmitter
Rx	:	Receiver
EIL	:	External Injection Locking
SIL	:	Self Injection Locking
LFF	:	Low Frequency Fluctuations
LEF	:	Linewidth Enhancement Factor
EDCL	:	External Cavity Diode Laser

OOK	:	On-Off Keying
PNA	:	Portable Network Analyzer
DCA	:	Digital Communication Analyzer
PRBS	:	Pseudo Random Bit Sequence
BERT	:	Bit Error Rate Tester
OSA	:	Optical Spectrum Analyzer
WDM	:	Wave Division Multiplexing
OFDM	:	Orthogonal Frequency Division Multiplex
UPD	:	Ultrafast Photodetector
NRZ	:	Non-Return to Zero
FWHM	:	Full Width at Half Maximum
SNR	:	Signal to Noise Ratio
PRBS	:	Pseudo Random Bit Sequence
QAM	:	Quadrature Amplitude Modulation
FEC	:	Forward Error Correction
TEC	:	Thermoelectric Cooler
SMSR	:	Side Mode Suppression Ratio
FWHM	:	Full Width at Half Maximum

ABSTRACT

Full Name : Md Hosne Mobarok Shamim
Thesis Title : Analysis of semiconductor laser diodes for high bit-rate visible light communication
Major Field : Electrical Engineering
Date of Degree : April 2018

Recently, the semiconductor light emitting diodes (LEDs) have taken center stage towards energy efficient indoor illumination, besides potentially offering high-speed Light Fidelity (LiFi) visible light optical wireless communication (VLC). On the other hand, visible semiconductor laser diodes (LDs) are now being considered as another promising solution for simultaneous illumination and communication, thanks to their high quantum efficiency and data transmission capacity compared to LEDs. In this work, we have investigated the dynamic characteristics of LDs via cost-effective self-injection locking scheme, particularly, the laser spectral linewidth and modulation bandwidth, which determines their direct modulation capabilities and hence the speed of VLC.

We have demonstrated self-injection locking on InGaN/GaN (blue/green) and InGaP/AlGaInP (red) visible laser diodes. The optical feedback path was accomplished via free space and employing a reflective mirror. The effect of injection current and optical power injection ratio on the spectral linewidth and modulation bandwidth of the lasers are investigated. Our results show that the laser performance could be substantially improved by employing this simple assisting technique. In particular, we achieved a significant increase of ~57% (1.53 GHz – 2.41 GHz) in the modulation bandwidth and ~9 times (0.63 nm to 0.07 nm) reduction in spectral linewidth. Consequently, side-mode-suppression-ratio

was considerably increased and enabled a single longitudinal mode operation, in green and blue lasers, respectively. This work paves the way for high speed optical wireless communications overcoming the challenges of limited modulation bandwidth and multi-mode operation of the visible laser diodes.

We also have employed our system to achieve high data rate in a VLC communication link. We have demonstrated 4 Gbps data rate using On Off Keying (OOK) modulation scheme, which is only limited by the bandwidth of the laser mount (1 GHz) and low sensitivity of the photodetector ($\sim 0.12 - 0.5$ A/W).

This work is a step towards addressing the future demand for high speed communication and various other applications.

ملخص الرسالة

الاسم الكامل: مد حسني مباروك شميم

عنوان الرسالة: تحليل ثنائيات ليزر أشباه الموصلات لتوصيل الضوء المرئي ذي معدل البتات العالي

التخصص: الهندسة الكهربائية

تاريخ الدرجة العلمية: إبريل عام 2018

في الآونة الأخيرة، الصمامات الثنائية الباعثة للضوء (LED) المصممة باستخدام أشباه الموصلات أصبحت من أهم وسائل الإضاءة الداخلية الموفرة للطاقة، كما أنها توفر إمكانية استخدامها في الاتصالات البصرية باستخدام الضوء المرئي (VLC). في المقابل، ليزر أشباه الموصلات (LDs) يمثل وسيلة أخرى للإضاءة والاتصال المتزامنين بفضل كفاءته الكمية وسعة إرسال البيانات بالمقارنة مع الصمامات الثنائية. في هذا العمل، تحرينا الخصائص الديناميكية لليزر أشباه الموصلات باستخدام طريقة ذات كفاءة مادية وهي التثبيت بالحقن الذاتي، بالأخص عرض الخط الطيفي وعرض نطاق التضمين الذي يحدد إمكانيات التضمين وبالتالي سرعة الاتصالات الضوئية المرئية.

عرضنا التثبيت بالحقن الذاتي باستخدام الليزر المكون من InGaN/GaN (اللونين الأخضر والأزرق) و InGaP/AlGaInP (اللون الأحمر). تم تحقيق مسار التغذية الرجعية في الهواء باستخدام مرآة عاكسة. تم التحقق من تأثير التيار المحقون ونسبة القوة البصرية المحقونة على عرض الخط الطيفي وعرض نطاق التضمين. نتأجنا توضح أنه بالإمكان تحسين أداء الليزر باستخدام هذه الطريقة البسيطة. بالتحديد، تمكنا من الوصول إلى زيادة كبيرة تصل إلى 57% (1.53 جيجا هيرتز – 2.41 جيجا هيرتز) في عرض نطاق التضمين وخفض عرض الخط الطيفي إلى تسع العرض الأصلي (من 0.63 نانو متر إلى 0.07 نانو متر). بالتالي، نسبة قمع الأنماط الجانبية تحسنت بشكل ملحوظ مما سمح بتكون نمط طولي واحد لليزر باللونين الأخضر والأزرق. هذا العمل يمهد الطريق للوصول إلى اتصالات بصرية ذات سرعات عالية والتغلب على التحديات المتعلقة بعرض نطاق التضمين وسليبيات التشغيل المتعدد النمط لليزر.

تم استخدام هذا النظام أيضاً لتحقيق سرعة نقل بيانات عالية باستخدام اتصالات الضوء المرئي. عرضنا معدل نقل بيانات يصل إلى 4 جيجا بت في الثانية باستخدام تضمين الإبدال بالفتح والغلق (OOK) المقيد بعرض نطاق منصة الليزر (1 جيجا هيرتز) والحساسية المنخفضة للكشاف الضوئي (0.12 - 0.5 أمبير لكل واط).

هذا العمل يمثل خطوة في الطريق لتلبية الطلب على اتصالات ذات سرعة عالية وتطبيقات أخرى عديدة

CHAPTER 1

INTRODUCTION

Fire and smoke is most probably the first demonstration of visible light communication (VLC) which has been used to share single messages like victory in the war or signaling any threat for thousands of years. In the years of early sea voyage, lighthouses were used to help navigating the sailors in the sea [1]. In 1880, Alexander Graham Bell and Charles Sumner Tainter invented Photophone where the light beam was modulated to send a voice signal wirelessly [2]. During the same time, James Clerk Maxwell mathematically predicted the existence of the electromagnetic radiation [3] which later experimentally proved by Heinrich Hertz in 1888 [4]. Sir Jagadish Chandra Bose of British India (Currently Bangladesh) was the first person to demonstrate a mm wave wireless data transfer in Town Hall of Kolkata in 1894 [4]. Italian Physicist Gulielmo Marconi later patented a similar invention, and thus the microwave communication started. In the twentieth century, the innovations and discovery in science and technology expanded exponentially, which led to the era of the radio frequency communication system. After the invention of the laser in 1958 [5] and light confinement technique in optical fiber [6] in 1966, we set foot in the age of high speed optical fiber communication. The technological booming gave birth to the internet at the end of 20th century which caused the data rate requirement to grow exponentially. The global internet traffic has been increased three times in last decades which is expected to increase even three times more in next five

years[7]. Eventually, we have created the optical fiber backbone around the globe to tackle this growing demand of high speed connectivity even though in consumer level, we are still trapped with microwave communication whose capacity is much lower than the optical communication. For indoor communication, visible light has been proposed as a mean of simultaneous illuminations and communication to overcome these shortcomings since the last decade. In this work, we will address the limitations of the visible laser as a transmitter in terms of bandwidth and linewidth and pose a possible solution using a self- seeded optical feedback technique.

1.1 Visible light communication

Visible light communication addresses the visible region of the electromagnetic spectrum as a mean of communication. Figure 1-1 [8] represents the visible spectrum of the spectrum which is ranged between 380 nm ~ 750 nm.

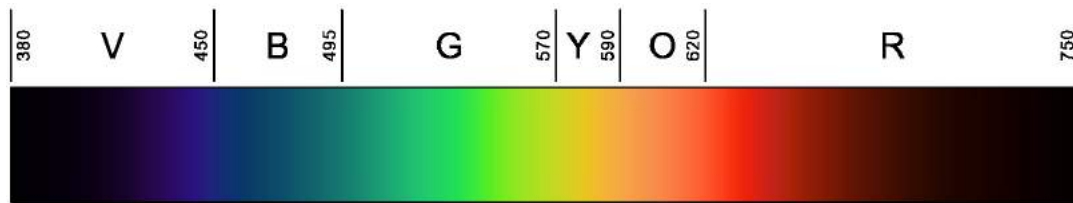


Figure 1-1 Visible portion of the electromagnetic spectrum. The ranges are marked in nanometer wavelength

Internet of things and smart cities are not very distant future where people are always connected to not only each other but also to the machines. These technologies will make our life more comfortable, but the price for that comfort is huge data traffic which our present infrastructure is not capable of handling. Although, we have high speed optical fiber internet backbone under the ocean, because of the limitations of radio frequency (RF)

technology, the low speed at the consumer end is posing a challenge. Thus, high data rates at the subscribers are required to step into the future, and visible light optical wireless communication has been identified as a promising solution. Advantages of VLC over the current RF network system are: un-regulated spectrum of wavelengths, no electromagnetic interference, higher security, higher data rate, lower power consumption, etc. Besides, VLC is such a technology where indoor illumination and high-speed communication in the form of LiFi (Light Fidelity) can be accomplished simultaneously, thus reducing the energy consumption to a great extent.

The essential elements of a visible light communication system consisting of a laser diode (LD) or light emitting diode (LED) as a transmitter and a photodiode as a receiver as shown in Figure 1-2.



Figure 1-2 Basic Elements in Visible Light Communication system

The transmitter converts the electrical signal to the optical signal, and the receiver does exactly the opposite. Modulating the transmitting signal directly or externally is necessary to establish any communication. A complete system would require few other passive components and active devices. Table 1-1 contains a list of such devices and components. Apart from these, some other optical parts like translational stage, diaphragm, post holders, etc. are necessary to ease the operation of the system.

Table 1-1 Elements of a visible light communication link

Active Devices	Passive Components
Laser Diodes/ LEDs	Beam splitters
Photodetectors (PIN, APD)	Lenses
Amplifiers	Fiber coupler

1.1.1 Transmitter

LASER stands for *Light Amplification by Stimulated Emission of Radiation* which is a source of coherent monochromatic radiation in the optical region ($0.2 \mu m \sim 20 \mu m$). It is analogous to an RF source or electronic oscillator that comprises of an amplifier and a feedback. The three main components of any laser are:

1. Gain Medium or the active medium
2. Pump or power supply
3. Optical resonator

When the active medium is pumped, it provides some gain whereas the resonator has some losses. Whenever the net gain exceeds the loss, the laser can start oscillating. A semiconductor laser is usually built on a direct bandgap semiconductor which radiates photons during recombination whereas for the indirect bandgap semiconductor phonon is being emitted. Population inversion facilitates the stimulated emission instead of absorption. Finally, an optical resonator provides a large photon density to enable a coherent stimulated emission which is known as Laser. In our work, we focus on

electrically pumped semiconductor laser diode only. A typical homojunction semiconductor laser structure is given in Figure 1-3. Semiconductor lasers are commercially available in a packaged condition whose top side is open thus named top open (TO) can.

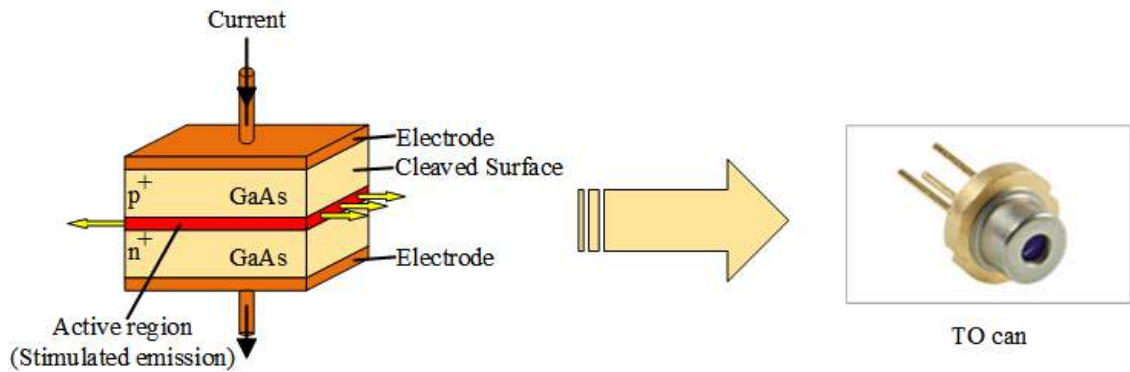


Figure 1-3 Basic structure of a homojunction laser diode (left) and a sample of commercially available TO can laser diode (right)

1.1.2 Receiver

Photodetectors (PD) are used as a receiver in VLC, and it converts the optical signal to the electrical signal. Commercially available photodetectors are usually of two types named PIN and Avalanche Photodetector (APD). The responsivity of the PIN PDs is lower than that of APDs. On the contrary, the APDs are limited with a very small modulation bandwidth. Both of these parameters have strong relation to the data rate of the VLC communication link.

1.2 Injection locking

Injection locking is a widely used technique to improve the linewidth, reduce the chirp, enhance the bandwidth, etc., of a laser. The intensity modulation frequency (-3 dB point of a modulation response) is approximately proportional to the relaxation oscillation frequency, $\omega_r = \sqrt{\frac{v_g a S_0}{\tau_p}}$. In this equation, v_g is the group velocity, a is the gain of the material, τ_p is the photon lifetime, and S_0 is the photon density of the laser diode. This equation suggests that increasing the modulation bandwidth can be done by injecting higher current which in turn heat up the system and reduce its performance. Wang *et al.* [9] suggested optical injection from another similar laser source called a master laser which can increase the intrinsic modulation bandwidth of the free running (slave) laser substantially by increasing the photon density in the active region.

1.2.1 External injection locking (EIL)

In external injection locking two similar type of lasers, a master, and a slave, are used as shown in Figure 1-4. The master laser needs to be carefully detuned near to the slave laser to lock a single longitudinal mode. An isolator is usually used in the system to avoid any interference of the light beam in the system. Finally, the beam from the slave laser goes to the measurement devices for characterization and communication or other applications.



Figure 1-4 External injection locking block diagram

1.2.2 Self-injection locking (SIL)

Using a mirror instead of an auxiliary master laser diode reduces the cost and complexity of the system as shown in Figure 1-5 preserving the potential to improve the laser quality. Throughout this thesis we will explore the behavior of the system under the Self-injection locking (optical feedback) scheme.



Figure 1-5 Self-injection locking block diagram

1.3 Research motivation

Although the modulation bandwidth (spectral linewidth) of LD is significantly higher(narrower) than the LEDs, various techniques have been utilized in the literature to improve the laser beam quality further as this fundamentally dictates the direct modulation capability of LD and hence the optical transmission capacity. For instance, Bragg gratings, distributive feedback, optical injection locking, etc., have been considered in near infra-red (NIR) based light sources to achieve almost single wavelength operation with transmission data rates in 10's of Gb/s using direct modulation scheme. In particular, optical injection locking is found to be an attractive assisting solution capable of offering not only higher output power but also almost single wavelength mode operation. Moreover, this technique is shown to reduce the frequency chirp of the LDs considerably and improves the direct modulation capability of the diodes, thus able to achieve high data rate and long-distance

communication, in C band wavelength. Two variations of injection locking techniques is reported in NIR regime; optical external injection locking and self-injection locking. While the former utilizes an external seeding high-quality laser (master) whose power is injected into a similar lower quality LD (slave) operating at similar wavelength for locking a particular wavelength Fabry-Perot mode of the laser, the later is based on feeding back part of the laser output power back into the device for locking purpose. Although external injection locking has been comprehensively utilized and the underlying physics is well understood in the NIR LDs, they are living in their infancy in the visible region with a handful of reports in the literature. On the other front, self-injection locking is highly attractive because of its cost-effective and energy efficient deployment (does not require an additional high-quality laser) and has been proposed as a potential candidate in next-generation NIR communication systems. However, this technique has not been reported in the literature, in the visible light region, to our knowledge. Therefore, in this work, we intend to explore self-injection locking on visible LDs with the aim of understanding the underlying physics and to enhance the bandwidth of these LDs for green high-speed VLC system.

1.4 Research objectives

The primary goal of this research module is summarized below:

1. Device characterization of the commercially available blue, green, and red TO-can semiconductor lasers diode in terms of lasing emission spectrum, L-I-V characteristics, and small-signal modulation response.

2. Perform the self-injection locking characterization of blue, green, and red semiconductor laser diodes. In particular, the effect of the following parameters will be compared between the free running and injection-locked lasers
 - a. Optical linewidth
 - b. Small signal modulation response.
 - c. Injection ratio
3. Perform ON-OFF Keying direct modulation on the self-injection locked visible semiconductor laser diodes and compare their performance with a free running counterpart, under an indoor free-space communication channel.

1.5 Research methodology

In order to execute the proposed work, off the shelf 450 nm, 520 nm, and 638 nm blue, green, and red laser from Thorlabs company have been employed for self-injection locking characterization and data transmission experiments. The block diagram is shown in Figure 1-6, and it is based on free space optics (i.e., mirrors to feedback the light into the laser, beam splitters, lenses, etc.). This work required few high-end sophisticated equipment like visible optical spectrum analyzer, the bit-error-rate tester, high-frequency pattern generator and digital communication analyzer which is unavailable in Electrical Engineering Department of KFUPM. Hence, facilities of Photonics Laboratory of King Abdullah University of Science and Technology (KAUST), which is well equipped with these equipments, was utilized in the transmission experiments. First, several devices were tested for lowest threshold current, high slope efficiency, and high output power, to select the best laser device, at room temperature. Later, the temperature dependent spectral analysis was

carried out for this device to be utilized in the locking experiments. After this phase, the self-injection locking set-up was built as shown in Figure 1-7. Moreover, variations in the setup were also tested to identify the best configuration for eventual transmission experiments and self-injection locking characterization. The short-term stability test of the locked mode, the mode power, and the side mode suppression ratio are some of the parameters that was evaluated in this characterization experiment. We also have tested the system under variable external cavity and injection ratio to understand more about the behavior of the laser.

Once, the characterization was completed, the transmission experiments using OOK scheme was carried out. In the transmission experiments, we examined the effectiveness of the laser diodes under self-injection locking scheme to perform high-speed data transmission.

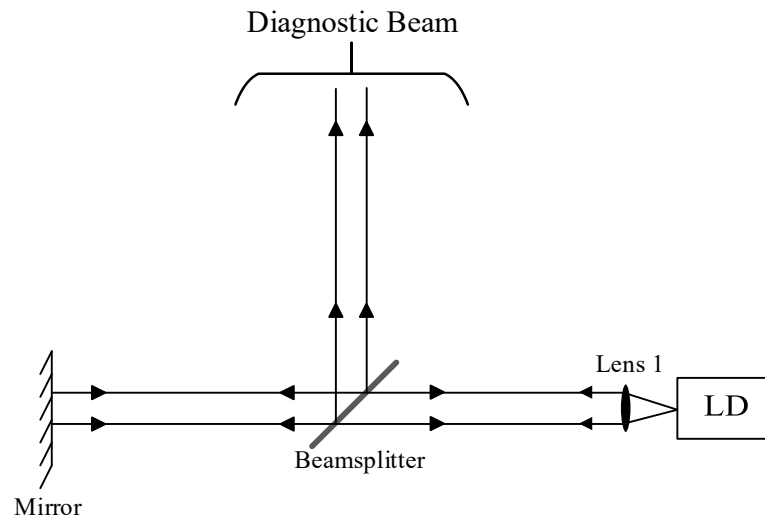


Figure 1-6 Block diagram of a free space self-injection locking setup

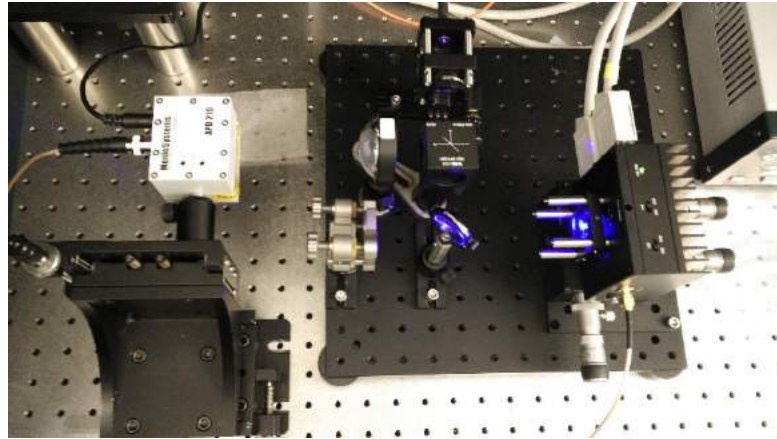


Figure 1-7 Laboratory photograph of the self injection locking setup

CHAPTER 2

DEVICE CHARACTERIZATION

In our experiment, we have used commercially available equipment, devices and parts including the transmitter laser diodes and the receiver photodetectors. In Table 2-1 the specification provided by the manufacturer are given for the blue, green, and red (BGR) laser diodes.

Table 2-1 Laser diode parameters obtained from the manufacturer [12]–[14]

Parameter	Blue	Green	Red
Emission Spectrum (<i>nm</i>)	440-460	510-530	628-648
Spectral Width (<i>nm</i>)	2	2	-
Threshold Current (mA)	30	45	45
Modulation Frequency (MHz)	>100	>100	>100

We have also characterized the laser diodes experimentally which will be presented in the subsequent sections. Since the lasers were class 3B, we also had all the necessary safety precautions including a proper enclosure for the whole setup as it is shown in Figure 2-1.



Figure 2-1 Safety enclosure for the experimental setup

2.1 450 nm blue laser diode

2.1.1 LIV characteristics

LIV is a significant characteristic for a laser diode from which we can extract the threshold current, threshold current density, optical power slope of the device, etc. It gives an overall idea about the device and its performance. The LIV measurement was taken at 20°C thermoelectric cooler (TEC) temperature at 8% ratio of the beamsplitter which was placed in between the external cavity. From Figure 2-2, the threshold current for the blue laser (PL450B, Thorlabs) was found to be 25.8 mA, which is in nice agreement with the manufacturer specifications. The slope efficiency, the ratio of the optical power output to the injection current, of the laser is 0.09 W/A. From the VI characteristics, we calculated

the dynamic resistance of the laser to be $\sim 7 \Omega$ at the saturation, as it was measured from Figure 2-3.

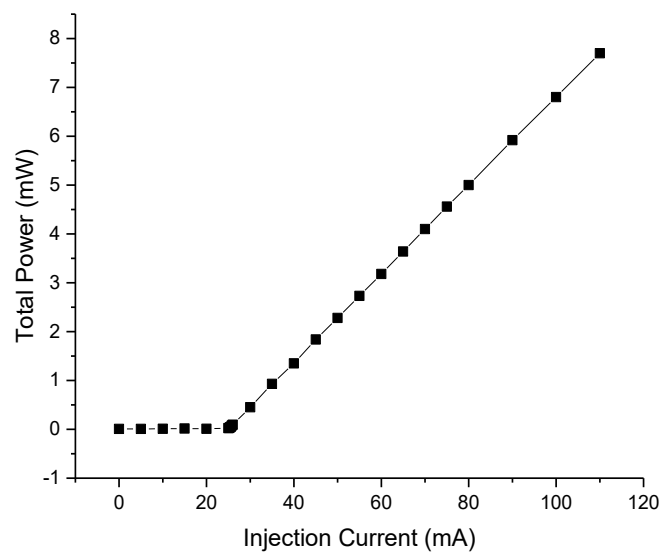


Figure 2-2 L-I characteristics of 450 nm blue TO can laser diode

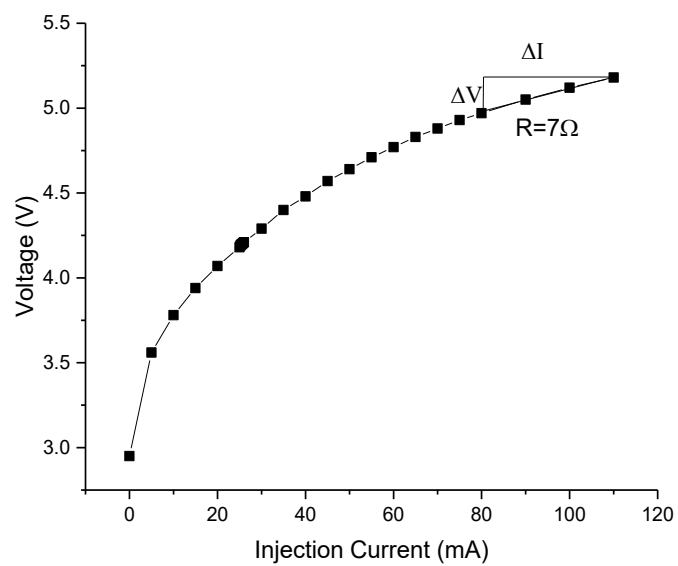


Figure 2-3 V-I characteristics of the 450 nm blue TO can laser diode

2.1.2 Lasing emission spectrum

The emission spectrum of the laser diode has been captured using optical spectrum analyzer (OSA, Yokogawa AQ6373B). The spectrum shifts to its right if the injection current is increased and vice versa. Also, the optical power emitted from the source increases proportionally with the applied injection current, maintaining the slope efficiency as shown in Figure 2-2. From Figure 2-4, it is evident that higher injection current causes the multi-longitudinal nature of the emission spectrum which is bad for long distance communication. At 20°C, the emission wavelength spans from 449.5 nm to 454.2 nm covering 4.7 nm. Due to the under developed material technology, the span of the wavelength is too low compared to the laser diodes at near infrared wavelengths. For the same reason, multi longitudinal mode is observed. Nonetheless, , single spatial mode lasers are available in the market already, in fact, our laser belongs to that group.

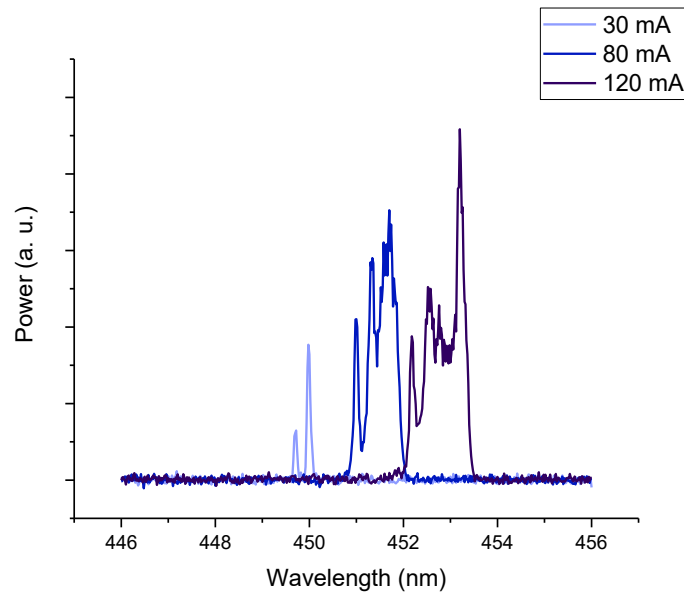


Figure 2-4 Emission spectrum of 450 nm blue laser diode at various injection currents

2.1.3 Small signal modulation response

From the small signal modulation frequency response, the performance of the large signal modulation in real communication can be predicted. A small sinusoidal wave at a fixed frequency is sent to the transmitter and received from the receiver and analyzed afterwards. To do that, we have used a 67 GHz portable network analyzer (PNA, Agilent E8361C) to measure the frequency response of the laser. Figure 2-5 represents the frequency response of the 450 nm blue laser diode at different injection current starting from just above the threshold. As the injection current increases, the -3 dB bandwidth begins to increase until a certain point. After that, it again reduces and saturates at higher injection. In this figure, we observe a dip in the frequency response because there was a problem with the laser diode mount. Without considering the dip, after 1 GHz, we can see that the bandwidth at 80 mA is quite higher than 30 mA. However, the difference is meager from 80 mA to 120 mA. Since the responsivity of the photodetector (UPD-50-UP) is very low 0.12 A/W in the blue region of the spectrum, we had to use another trans-impedance amplifier (Tektronix PSPL5865) after the UPD to enhance the received signal. The measurement of the bandwidth at different injection currents will be presented in Chapter 3 while comparing the performance with respect to the self-injection locked laser.

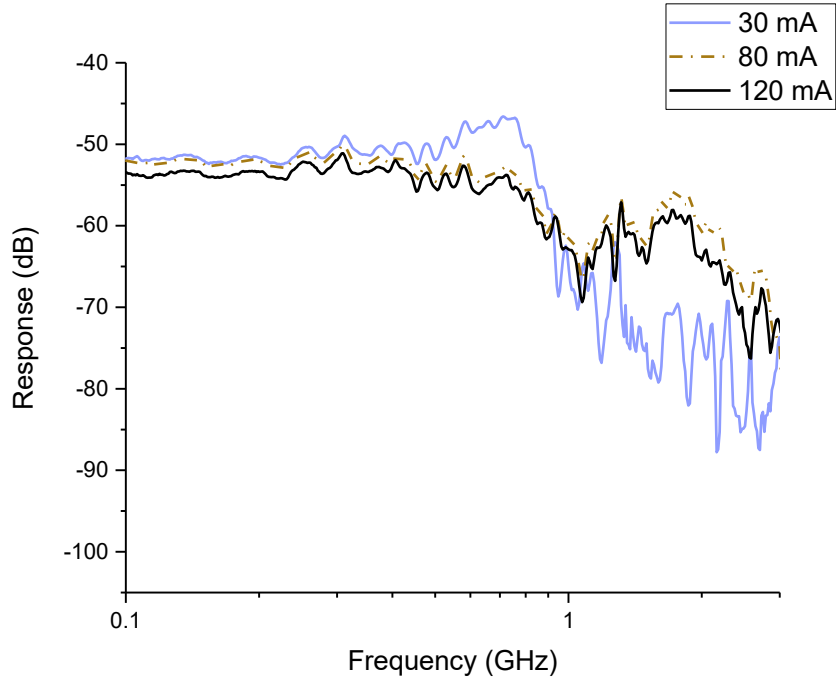


Figure 2-5 Small signal modulation of 450 nm blue laser diode

2.2 520 nm green laser diode

2.2.1 LIV characteristics

Figure 2-6 and Figure 2-7 represents the L-I and V-I curves for the 520 nm green laser diode. The threshold current was observed as 34 mA. The slope efficiency is 0.0627 W/A, close to that of the blue laser used in this experiment and the measurement was taken at the 8% of the light beam from a pellicle beamsplitter. The resistance imposed by the laser is 3.75 Ω , almost half of the blue laser.

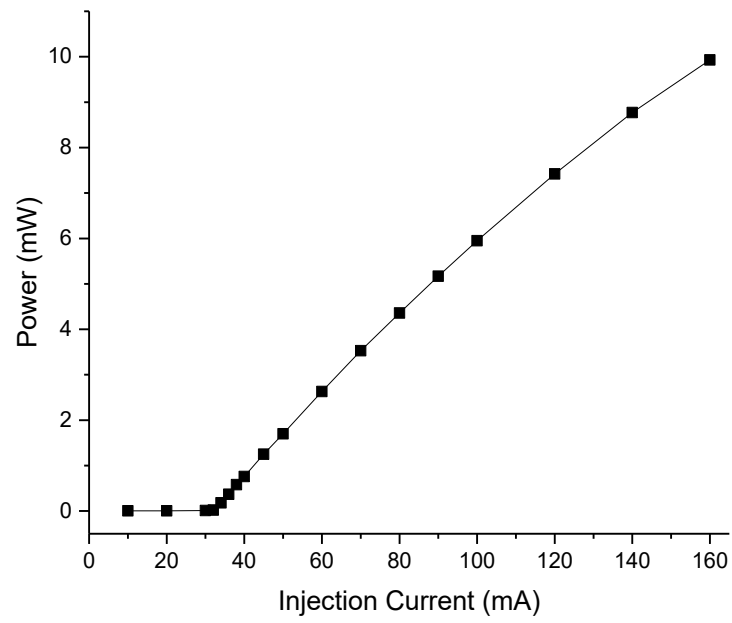


Figure 2-6 L-I characteristics of 520 nm green laser diode

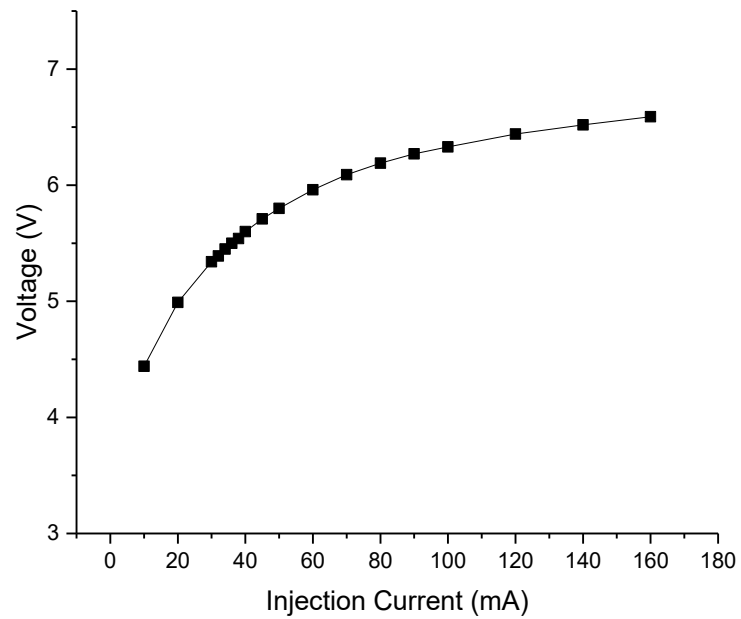


Figure 2-7 V-I characteristics of 520 nm green laser diode

2.2.2 Lasing emission spectrum

Since the green and blue laser diodes use the same kind of material technology, i.e., GaN, the behavior of the lasers is also similar. We observe the appearance of multi-longitudinal mode in case of green laser with the increase of injection current, which is similar to the blue laser. The linewidth of both lasers is around 1-2 nm. The span of tunability of the emission with the help of injection current is 2.88 nm at a fixed temperature.

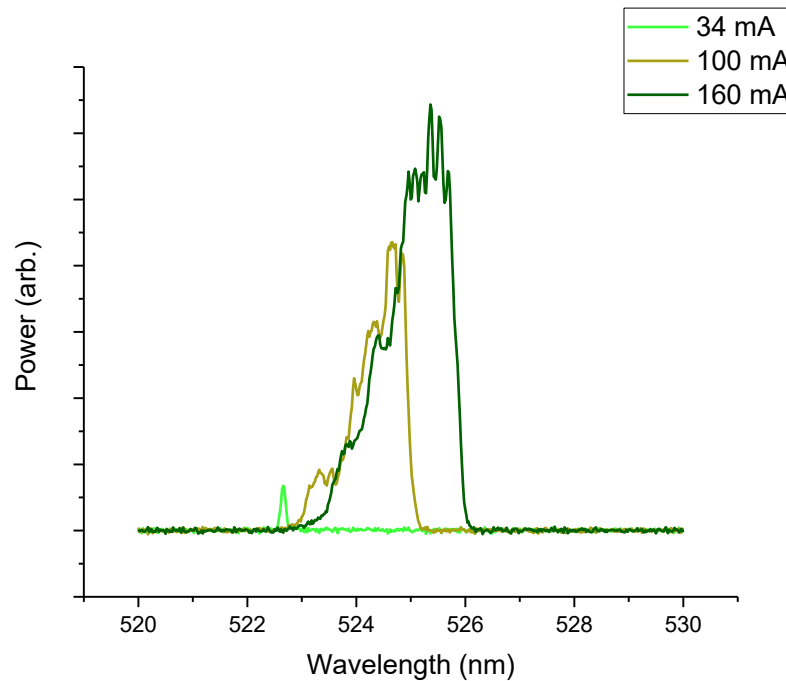


Figure 2-8 Emission spectrum of 520 nm green laser diode at various injection currents

2.2.3 Small signal modulation response

Figure 2-9 represents the frequency response for the green laser diode. Similar to the blue laser diode the modulation bandwidth is increasing with injection current until a certain point. At higher injection current the modulation response starts to reduce and saturates.

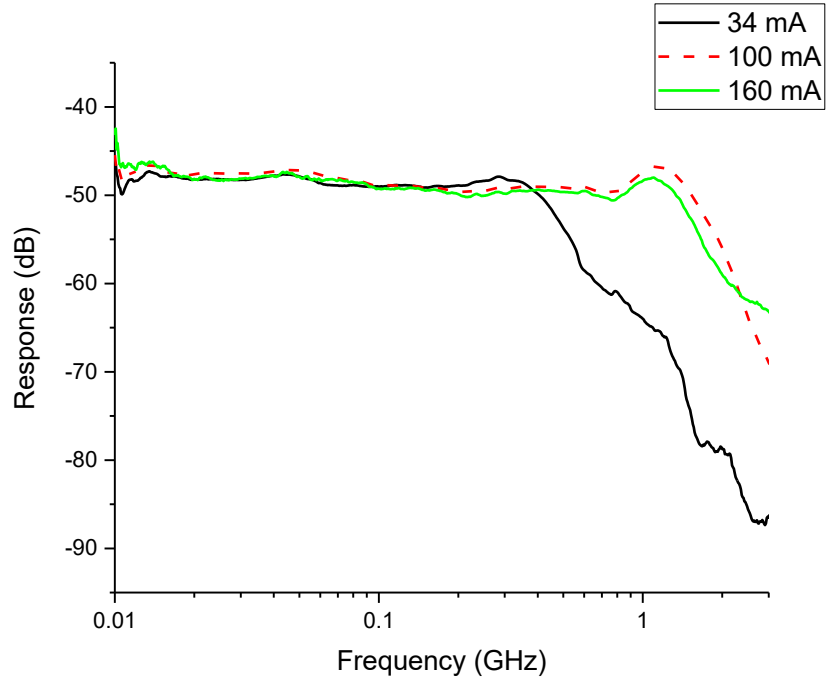


Figure 2-9 Small signal modulation of 520 nm green laser diode at various injection current

2.3 638 nm red laser diode

2.3.1 LIV characteristics

From the L-I curve of Figure 2-10, we see that the threshold current of the red laser is 42.7 mA. The slope efficiency is measured to be 0.015 W/A at 8% of the beamsplitter which is acting as the diagnostic beam. The resistance at the laser was observed from Figure 2-11 to be 7.5Ω , and it was very consistent throughout all the injection current. This consistency is perhaps due to the stable material technology of the red laser diode.

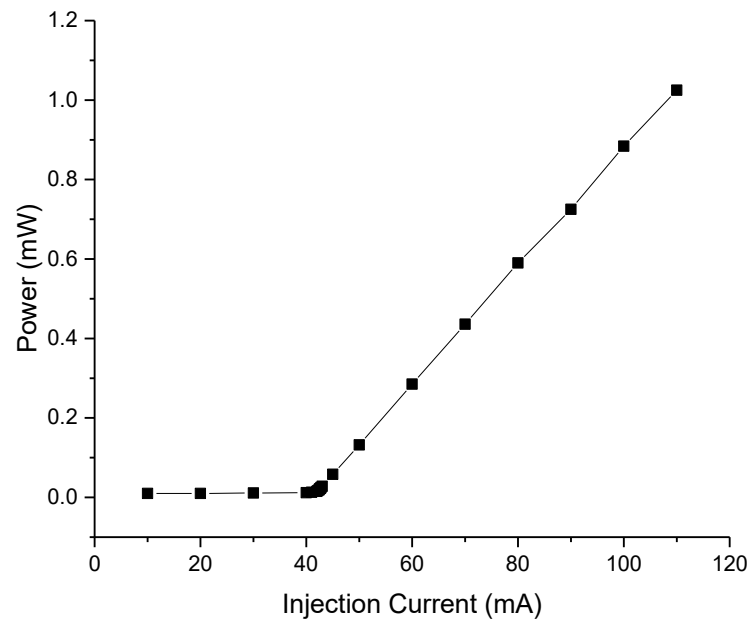


Figure 2-10 L-I curve for 638 nm, red laser diode

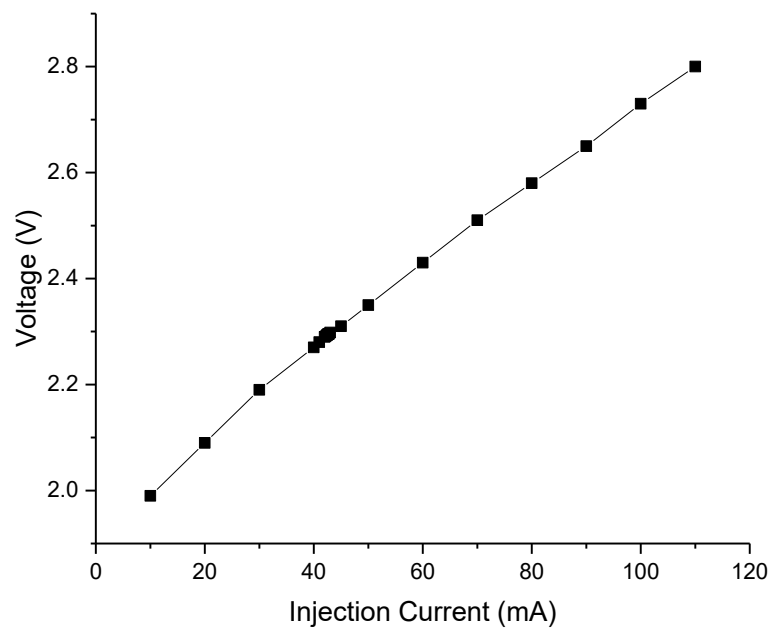


Figure 2-11 V-I curve of the 638 nm red laser diode

2.3.2 Lasing emission spectrum

The emission spectrum from the red laser has been shown in Figure 2-12. The linewidth across the spectrum is quite narrow and around 0.3 nm to be exact. It is very narrow compared to the blue and green GaN/InGaN laser counterparts. The span of the wavelength at a fixed temperature is around 3 nm.

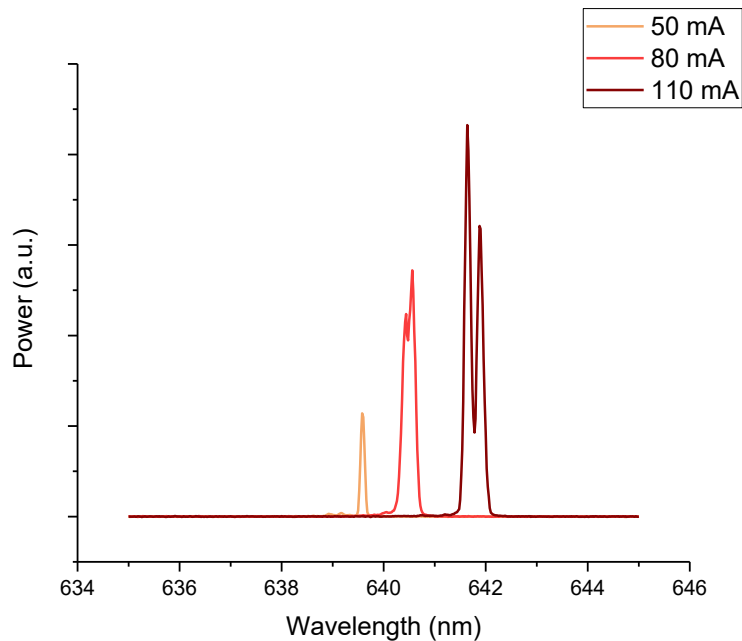


Figure 2-12 Emission spectrum of 638 nm red laser diode

2.3.3 Small signal modulation response

The effect of the injection current on small signal modulation is similar to the blue and green lasers except for the fact that it is much smoother and more stable. The bandwidth of the laser exceeds 2 GHz and only limited by the laser diode mount capacity.

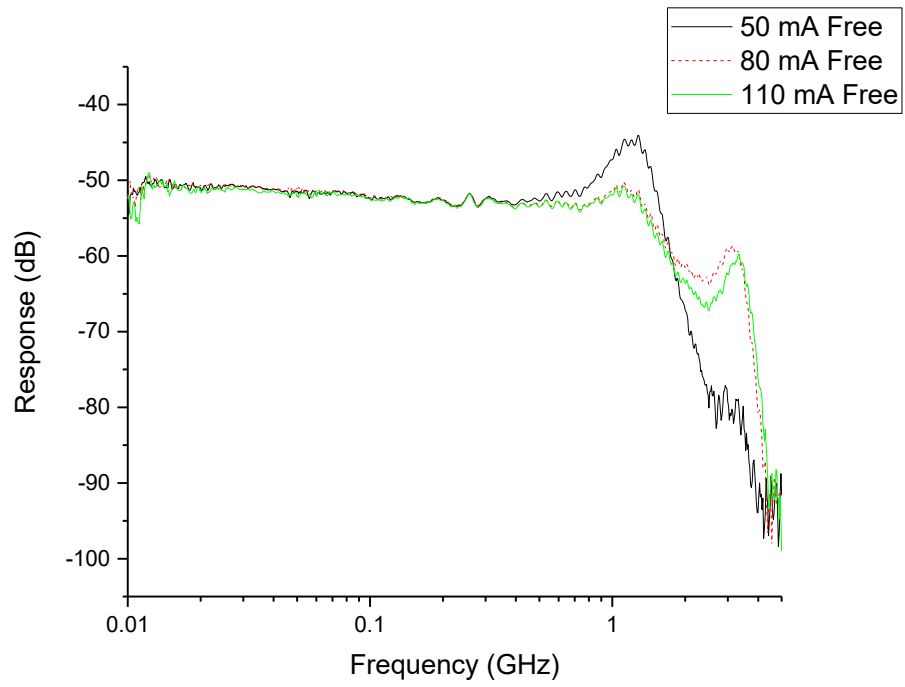


Figure 2-13 Small signal modulation of 638 nm red laser diode

CHAPTER 3

SELF-INJECTION LOCKING CHARACTERIZATION

Non-linear semiconductor laser dynamics due to optical injection, both EIL and SIL has been studied consistently since last four decades. Most of these works are theoretical and computer simulations [15], [16], [25]–[30], [17]–[24] in the near infrared region (NIR). Lang *et al.* [31] in his paper investigated the dynamic stability of the laser under weak to moderate optical feedback and showed that the laser can undergo mode hopping under certain conditions. Besides, he experimentally observed the hysteresis of the refractive index with respect to the frequency and the optical power with the increase of the injection current. Tuning of the external cavity changes the phase of the optical feedback. The model of the transient dynamic behavior stated in the paper is famously known as the Lang Kobayashi or LK model in short. Based on this model several studies like transient analysis of low frequency fluctuations (LFF) [24] and modulation bandwidth enhancement using strong optical feedback [9] was done. To formulate a design guideline for lasers with high endurance, Peterman [17] made a comprehensive theoretical study on the effect of the optical feedback on a single mode semiconductor laser diode. His study was based on the weak reflections coming from the fiber pigtails or optical connectors. He suggested that the mode hopping phenomenon is due to the reduction of the gain threshold and formation of the external cavity modes. Moreover, his paper theoretically describes the gain change phenomenon and how it affects the change of the refractive index of the gain medium in

terms of linewidth enhancement factor (LEF). According to his model, spectral linewidth (in wavelength domain) is inversely proportional to the injection ratio. He mathematically showed that a considerable linewidth reduction is possible when the round trip phase of the optical feedback is zero. Moreover, the fluctuation in the linewidth narrowing is a periodic behavior as suggested in LK model [31]. Finally, a very important but often ignored phenomenon of longitudinal mode splitting was addressed in this paper. He claimed that, at high injection ratio, the longitudinal split modes becomes very narrow and unstable. It induces a significant phase noise and intensity noise. The frequency of the intensity noise is very low which leads to the LFF.

A recent theoretical study has been done by Moustafa Ahmed *et al.* [27] where the LK model has been modified for strong optical feedback considering five round trips of the reflections assuming the system operating at $1.55 \mu m$. They had used the Rungee Kutta method for the numerical simulation of 0.25 cm external cavity system whose targeted modulation frequency improvement was 60 GHz from 14 GHz. Although, with a strong optical feedback they were able to generate a peak at around 55 GHz, there was a valley of -10 dB created on the way to the relaxation oscillation. They have also observed that the peak of the response becomes higher and narrower with the higher injection ratio of the optical feedback.

A similar recent study has been done by Grillot *et al.* on a quantum dot laser [26] where they studied the modulation properties of the semiconductor laser diode. They compared the self-injection as an external-injection when the master laser detuning is zero. They also came up with the conclusion that the increase of the injection ratio helps in increasing the modulation bandwidth. They were able to attain a 1.5 times improvement in the modulation

bandwidth than the solitary laser. They also have argued that longer external cavity doesn't show any improvement in the modulation bandwidth instead creates some ripples in the response. The dependency of the amplitude of the ripples on the coherence length of the laser was another unique finding from this paper. Finally, they showed that the higher LEF leads to higher modulation bandwidth along with a higher peak amplitude of the frequency response.

In [21], the authors experimentally characterized a commercial laser of wavelength 837 nm for a short external cavity of 5 cm and 1.1 cm. They have discussed the importance of the phase of the optical feedback. They identified a similar periodic behavior due to the periodicity of the phase of the optical feedback as mentioned above. Since the phase change could be complicated in an experiment, they have suggested using a piezoelectric transducer to tune the external cavity, else, change in the emission spectrum by tuning the injection current should also work.

Modulation bandwidth of a semiconductor laser diode is limited by the slow carrier photon (CP) interaction in the active medium. To improve the modulation bandwidth, strong external injection locking was applied in a 1557 nm single section distributive feedback laser having an adjacent integrated feedback section to the laser system which creates a photon-photon (PP) resonance in a particular frequency depending on the external cavity length [23]. They have identified the spectrally neighbored longitudinal modes to be the reason of the modulation enhancement even though the response is not flat and not suitable for the high speed communication. Later, a comprehensive study of external injection locking has been done on a 1550 nm VCSEL where the bandwidth could be tuned as they have detuned the wavelength of the master laser [22]. This technique has been used for

high speed free space optical communication in [32], [33] and visible light indoor communication in [34]–[37].

3.1 Self-injection locking experimental setup

The schematic of the experimental setup and the corresponding laboratory photograph are shown in Figure 3-1 (a) and (b), respectively. Here, the mirror serves as mean for optical feedback creating a free space external cavity. The green (red) lines correspond to the optical (electrical) path, and the yellow arrows show the direction of the light propagation. We used commercially available 450 nm (Thorlabs PL450B, blue), 520 nm (Thorlabs L520P50, green), and 638 nm (Thorlabs L638P040, red) TO-can single spatial mode laser diodes as transmitter sources. The coherent transmitted light-beam from the laser diode was collimated using an aspheric lens L1 (Thorlabs A110TM-A) of focal length 6.24 mm. An uncoated 92:8% pellicle beam-splitter BS1 (Thorlabs BP107) was used to facilitate simultaneous self-optical feedback and performance measurement. The 92% of the optical power was allowed to transmit towards a silver coated mirror (Thorlabs PF10-03-P01), which forms one end of the ~26 cm long external cavity. The mirror is selected to have high reflectivity of $> 97.5\%$ in the visible region, to ensure strong optical feedback into the edge-emitting laser's front facet that concludes the other end of the external cavity. To adjust the power injection ratio, we have used a compact neutral density filter (Newport FR-CV-75) in the external cavity to control the feedback optical power. The other 8% of the optical power from BS1 was again split with an identical 92:8% beam-splitter (BS2), thus enabling characterization of spectral linewidth via an optical spectrum analyzer (OSA,

Yokogawa AQ6373B with 0.02 nm resolution) at the 8% of the optical power, and modulation bandwidth via an ultra-fast photodiode (Alphas UPD-50-UP) at the 92% of the optical power. The responsivity of the UPD at 450 nm, 520 nm, and 638 nm are ~ 0.12 A/W, 0.25 A/W, and ~ 0.5 A/W, respectively, which is too low for the detection of the small portion of the light beams. Hence, a 26 dB linear amplifier (Tektronix PSPL5865) was incorporated in the system after the UPD to amplify the received optical power before sending it to the 67 GHz Network Analyzer (Agilent E8361C) to observe the modulation bandwidth. In our setup, ~ 18 cm distance between L1 and UPD is the free-space channel link. All the measurements were at room temperature of 20°C via a temperature controlled built-in heat sink of the laser mount (Thorlabs TCLD M9). To determine the power injection ratio, we measured the optical power of the laser after L1 using a calibrated Si photodetector (Newport 818-SL) and then estimated the feedback optical power considering all the losses due to external cavity length, beam-splitter, mirror, and the laser front-facet.

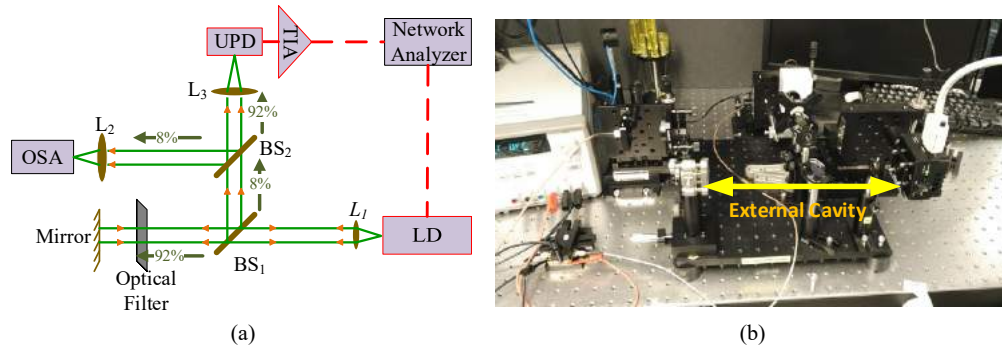


Figure 3-1 (a) Schematic of the self-injection locking experimental setup. (b) Laboratory photograph of the experimental setup.

3.2 LIV characteristics of Self-injection locked laser diodes

Figure 3-2, Figure 3-3, and Figure 3-4 illustrates the optical power and voltage characteristics versus the injection current (L-I-V) for the blue (450 nm), green (520 nm), and red (638 nm) (BGR) color semiconductor laser diodes under both, free-running and self-injection locked cases. The threshold current of the laser diodes in the free-running case, corresponding to 25.8 mA, 34 mA, and 42.7 mA is found to reduce to 25.4 mA, 33.7 mA, 41.9 mA in the self-injection locked case. This reduction in the threshold current is considered as a key signature of successful self-injection locking and has been previously observed in [38] and [39]. This phenomenon is attributed to the change in the gain threshold due to the difference in the localized refractive index in the active region of the laser [40]. The new gain, g_c , required for the laser to turn-on can be significantly smaller from the solitary threshold gain, g_{th} , depending on the power injection ratio, R and the phase of the optical feedback, ϕ_{ext} , as described by equation 3.1.

$$g_c = g_{th} - |C| \left(\frac{2\sqrt{R}}{L} \right) \cos(\phi_{ext}) \quad 3.1$$

Here, C is the coupling efficiency that depends on the reflectivity of the front laser facet from where the feedback optical power is re-injected. Hence, from Eqn 3.1, and under phase matching condition ($\phi_{ext} = 0^\circ$) of the optical feedback (which we accomplished by fine tuning of the external laser cavity length), g_c is expected to reduce. However, the V-I curve does not shows any notable change before and after the self injection locking.

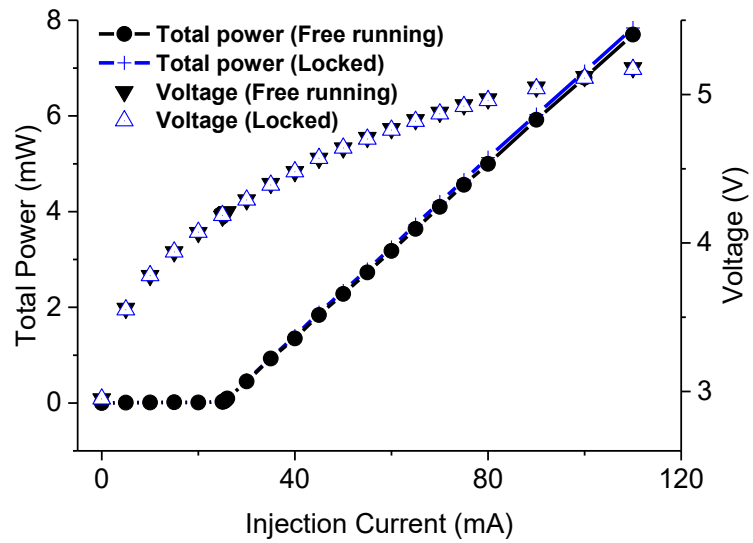


Figure 3-2 Comparison of the optical power and voltage characteristics of blue laser diode versus injection current, under the free running and self-injection locked cases.

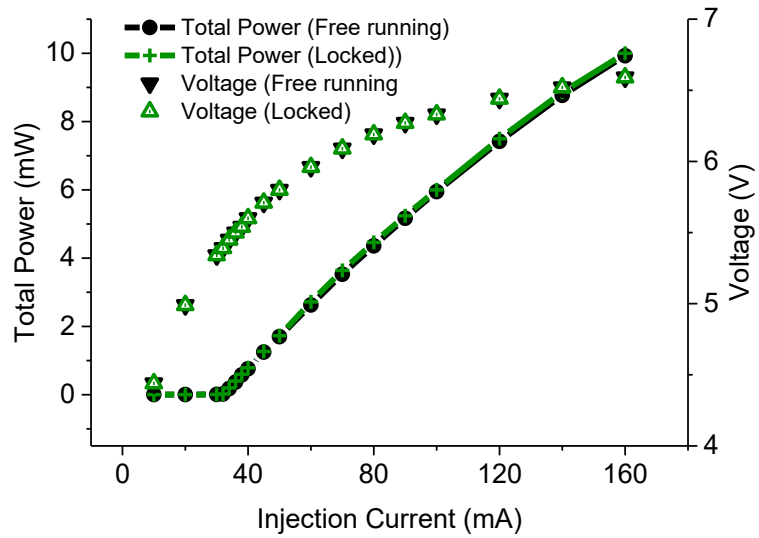


Figure 3-3 Comparison of the optical power and voltage characteristics of green laser diode versus injection current, under the free running and self-injection locked cases.

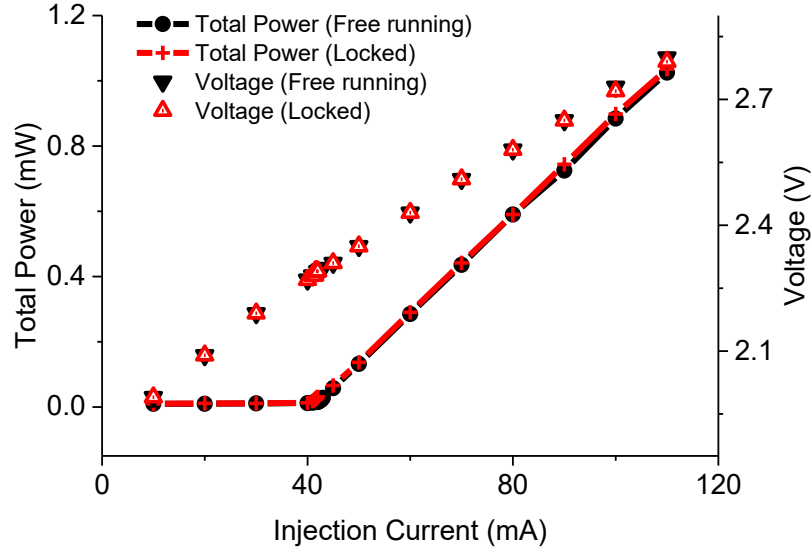


Figure 3-4 Comparison of the optical power and voltage characteristics of red laser diode versus injection current, under the free running and self-injection locked cases.

3.3 Emission spectrum of Self-injection locked laser diode

A particular Fabry-Perot mode is locked when it is sustainable in both the laser cavities (external and internal) [41]. FP mode spacing of the external cavity, which is calculated from equation 3.2:

$$\Delta\lambda = \frac{\lambda_c^2}{2nL_{ext}} \quad 3.2$$

is found to be ~ 0.4 pm ($\lambda_c = 450$ nm for blue), ~ 0.5 pm (523 nm for green), and ~ 0.8 pm (and 641 nm for red) for a cavity length, $L_{ext} \approx 26$ cm and refractive index, $n = 1$ is approximately three orders of magnitude smaller than the laser cavity mode spacing of ~ 0.3

nm (blue), ~ 0.25 nm (green), and ~ 0.15 nm (red), obtained from the corresponding lasing spectrums. The wavelength of the locked FP is essentially dictated by the laser cavity mode spacing. It is noteworthy to mention that fine tuning (micrometer range) of the external cavity is essential to match the phase of the optical feedback power of a particular FP mode in order for that mode to be injection locked, else mode hopping phenomenon occurs, which has been observed previously in the literature [39]. After careful tuning of the external cavity, a stable, single, locked FP mode was observed in blue, green, and red (BGR) laser diodes, which are shown in Figure 3-5, Figure 3-6, and Figure 3-7, respectively. The free running spectrum of the laser diodes are also plotted in the same figure for comparison purpose. We observe that the peak power of the locked FP mode increased significantly, thanks to suppression of the side modes (improved side-mode-suppression-ratio, SMSR) which enabled consolidation of the energies from the side modes into the single dominant longitudinal mode. This subsequently reduced the spectral linewidth (measured at the full-width-at-half-maximum, FWHM, considering the complete lasing spectrum).

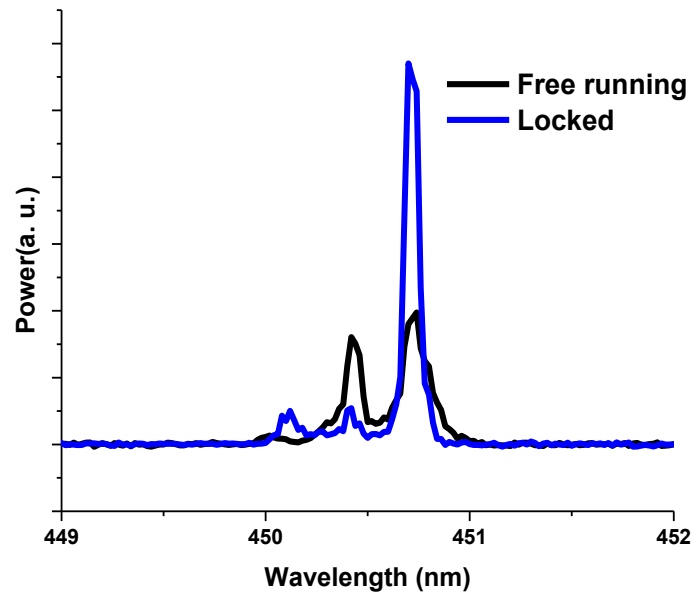


Figure 3-5 The lasing spectrum under self-injected locked and free running case for blue laser diodes.

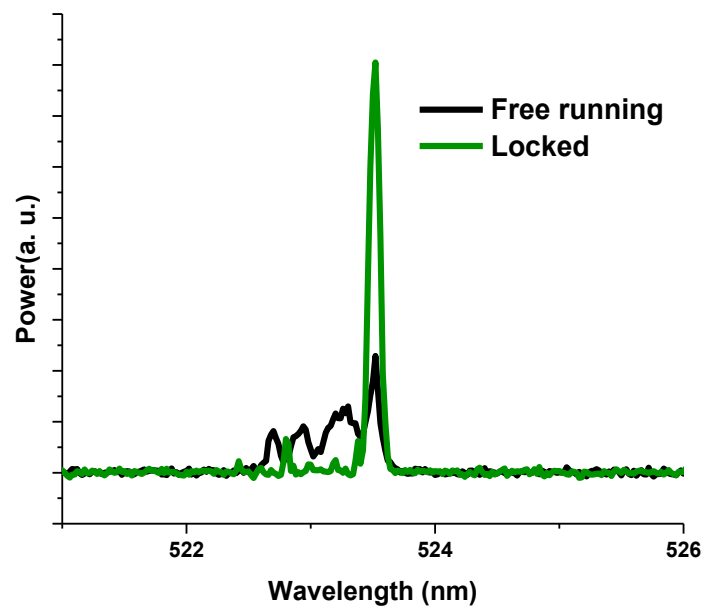


Figure 3-6 The lasing spectrum under self-injected locked and free running case for green laser diodes.

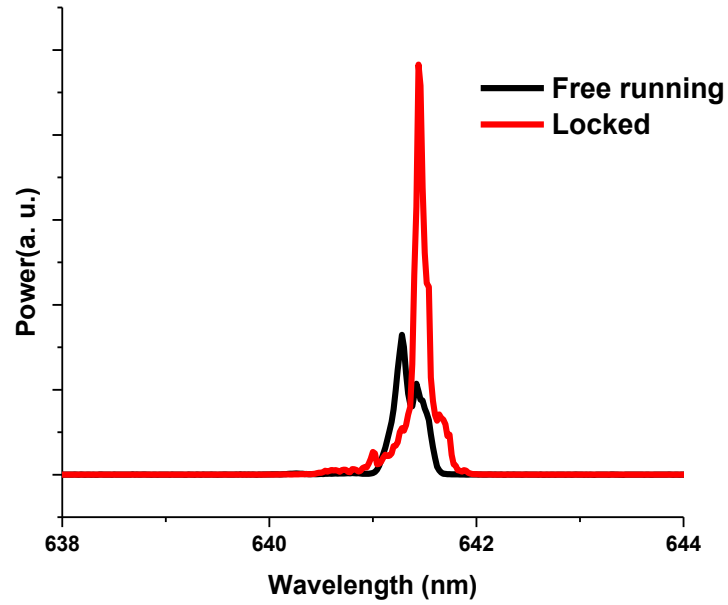


Figure 3-7 The lasing spectrum under self-injected locked and free running case for red laser diodes.

3.4 Small signal modulation of Self-injection locked laser diode

Small signal modulation for blue laser diode was carried out at 70 mA injection current, and 26 cm external cavity length. Modulations in the frequency response curves of Figure 3-8, Figure 3-9, and Figure 3-10, forming peaks and valleys, is observed in the locked cases, while a typical curve is observed for the free running case. This is attributed to the external cavity formation under SIL in the system. In fact, the difference between any two consecutive peaks is ~ 249 MHz or 560 MHz which is in excellent agreement to the calculated frequency spacing of ~ 268 or 548 MHz for the ~ 56 or 26 cm external cavities, i.e., $\Delta\nu = \frac{c}{2nL}$, where c is the speed of light, $n = 1$ and $L = \sim 56$ or 26 cm are the refractive index and length of the external cavities, respectively. Moreover, a considerable

improvement in the system response by 3.5–6 dB is also observed in green laser diodes, thus potentially facilitating higher direct modulation data transmission. The fluctuations in the frequency responses at lower frequencies are consistent with the literature, and has been termed as ‘Low frequency Fluctuations (LFF) [42]. Besides, a stable locking region with injection ratio > -10 dB [43] has been observed to be possible under LFF, which is exactly what has been observed in our case.

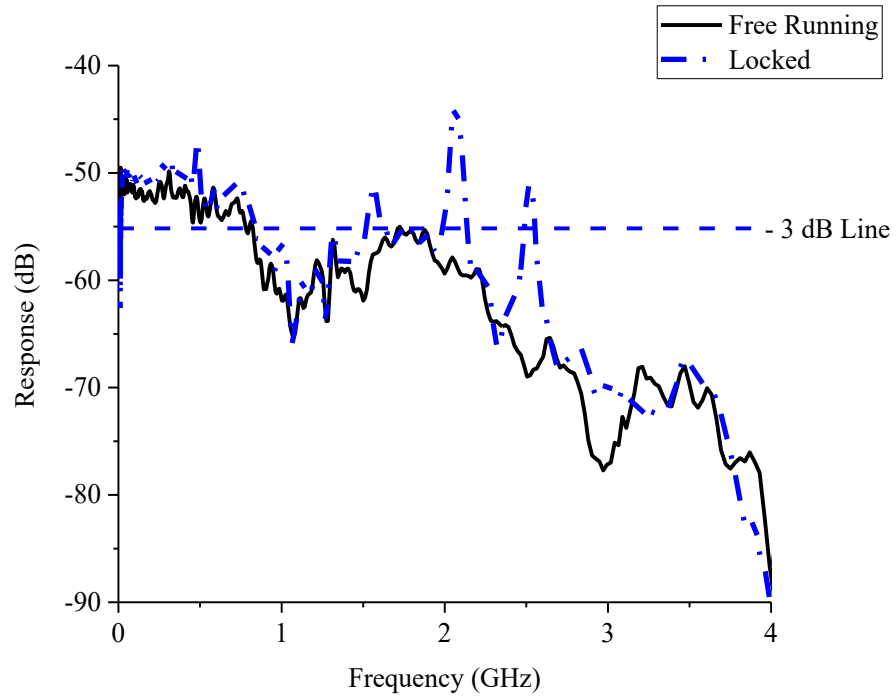


Figure 3-8 The small signal modulation response of 450 nm laser diode in free running and the injection locked case.

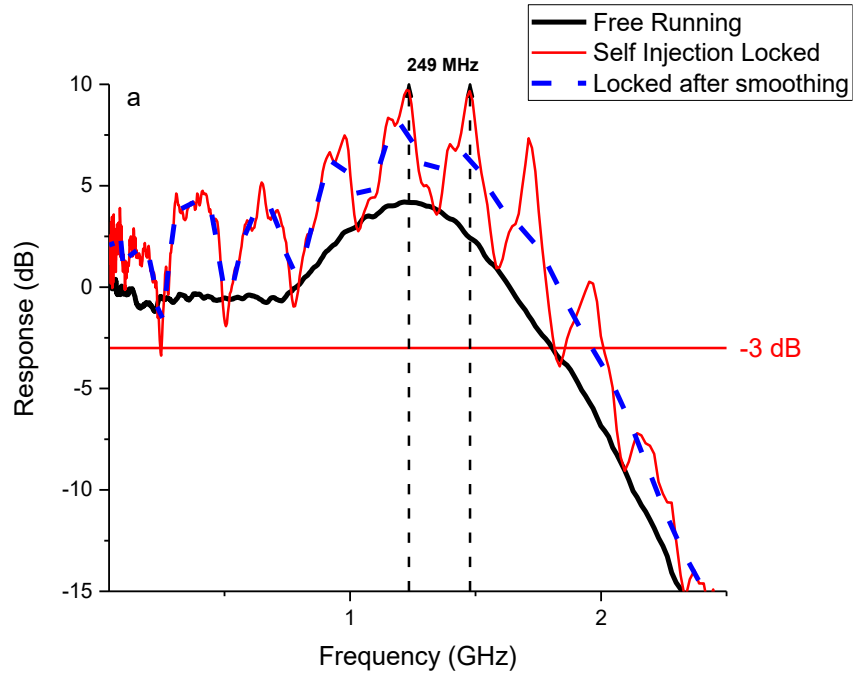


Figure 3-9 Frequency response of 520 nm green laser diode comparing the response of a solitary laser with the self injection locked laser.

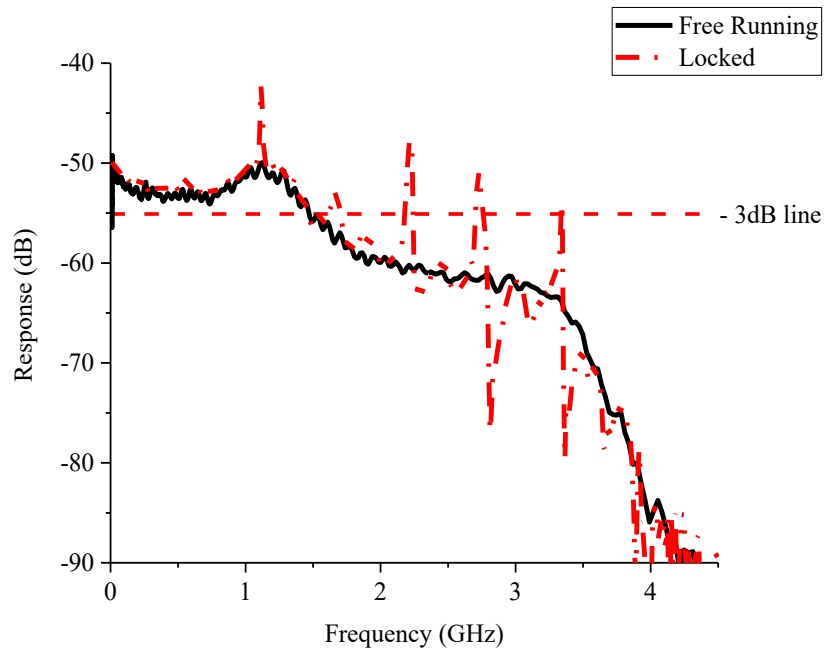


Figure 3-10 The small signal modulation response of 638 nm red laser diode for the free running and the injection locked case.

3.5 Stability of the Self-injection locking

A short-term stability test is initially performed on the self-injection locked laser diodes at a fixed injection current to ascertain steady operation of this assisting scheme in the visible region. Figure 3-11 (a) – (f) depicts the variation in total (integrated) optical power, peak power, peak wavelength, and SMSR of the self-injection locked mode of the BGR lasers along with the free-running counterpart, over a span of 20 minutes with 2 minutes interval. The injection currents for the blue, green, and red lasers are selected to be 54, 120, and 102 mA, respectively. In general, the stability of total power and peak power of the locked BGR laser diodes (Figure 3-11 (a) – (c)) are found to be comparable to the free running case or better, particularly for the red laser. Moreover, in all the cases, the self-locked power (total and peak) was found to be higher than the free running case, a signature of injection locking which has been discussed comprehensively in the earlier section. Referring to Figure 3-11 (d) – (f), which plots the variation of peak locked mode wavelength and SMSR, again exhibited comparable or superior performance from the injection-locked lasers compared to free-running case and across the entire time span, mainly for green and red lasers. Note that remarkable achievement of ~ 20 dB SMSR is measured from self-injection locked blue laser, which, to the author's knowledge, is one of the best values ever reported [44]. Comparable total power and the peak power values of this laser diode suggests close to single mode operation. Alternatively, green and red laser diodes exhibited SMSR values of ~ 6 and ~ 8 dB, respectively. In general, utilizing self-injection locking scheme on BGR

laser diodes improved the performance characteristics while preserving their stability with time, which is crucial for deployment in optical communications.

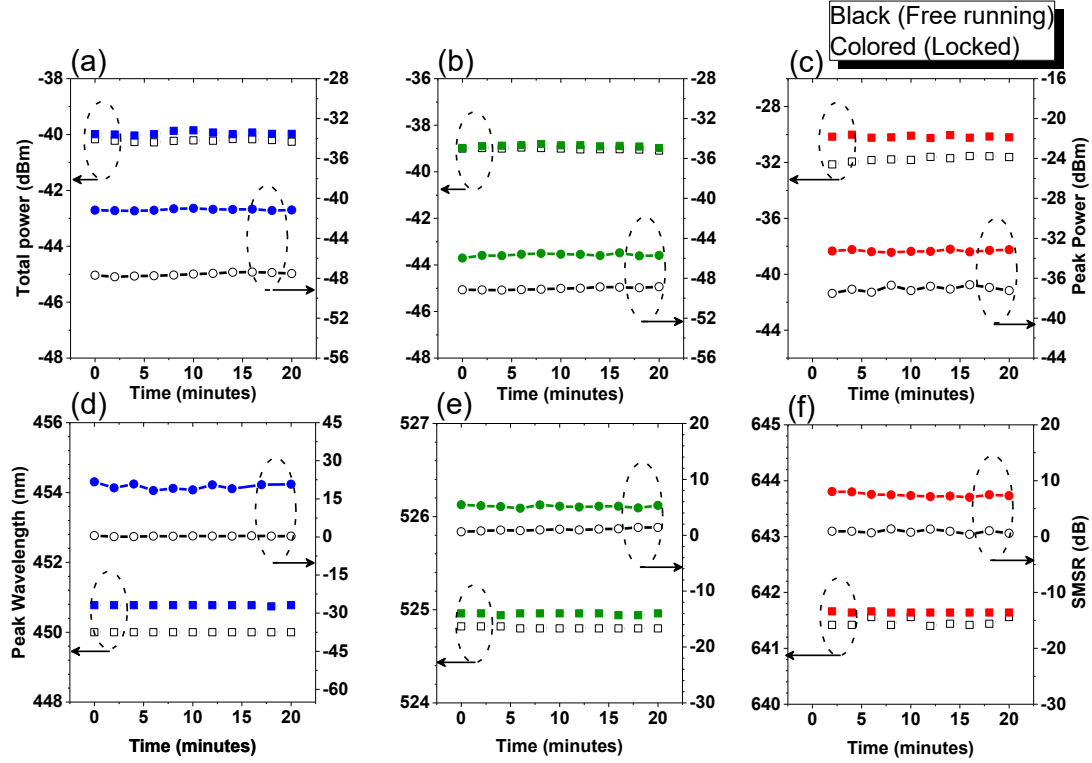


Figure 3-11 Short-term stability analysis of (a) and (d) blue, (b) and (e) green, and (c) and (f) red self-injection locked laser diodes.

3.6 Effect of injection current on Self-injection locking

Small signal modulation response of the BGR laser diodes has been performed to identify their transmission capacity under direct modulation. Figure 3-12, Figure 3-13, and Figure 3-14 plots the measured -3 dB bandwidth results for the free running and self-locked scenarios and under different injection currents. Considering blue and green laser diodes, a similar modulation bandwidth variation trend is observed with trivial change at low injections (up to $\sim 2.0 I_{th}$), substantial improvement at medium injections and again

inferior enhancement at higher injections. This is considered a typical laser diode behavior since its performance degrades at higher injection, and so is the frequency response [45]. A maximum of ~ 1.37 times ($\sim 28\%$) and ~ 1.57 times ($\sim 57\%$) improvement in modulation bandwidth is observed from blue (green) laser diode at 70 (120) mA injection current which corresponds to ~ 400 and ~ 880 MHz improvement, reaching a value of 2.18 (1.7 GHz under free running) and 2.41 GHz (1.53 GHz under free running), respectively. Alternatively, red laser diode showed ~ 270 MHz ($\sim 14\%$) improvement in the modulation bandwidth at 60 mA and displayed a similar trend of the bandwidth performance curve, as shown in Figure 3-14. Hence, these results show the effectiveness of this simple technique in substantially improving the laser direct-modulation capability, thus, contributing to the possible achievement of high bit-rate visible optical wireless communication.

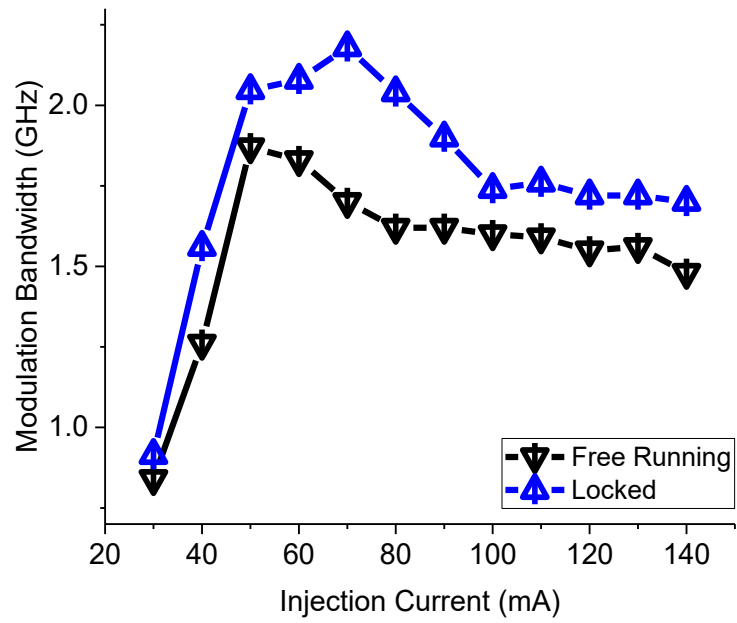


Figure 3-12 Variation of the modulation bandwidth as a function of injection current for blue laser diodes.

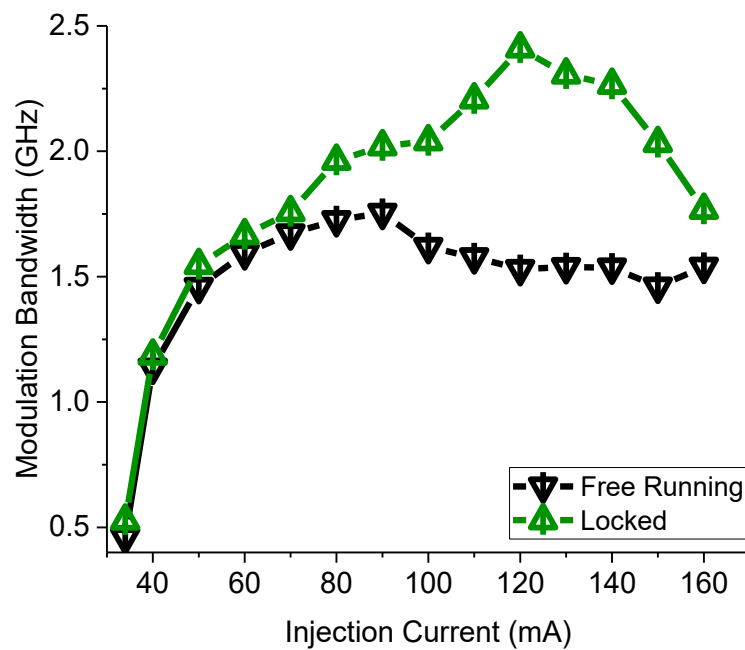


Figure 3-13 Variation of the modulation bandwidth as a function of injection current for green laser diodes.

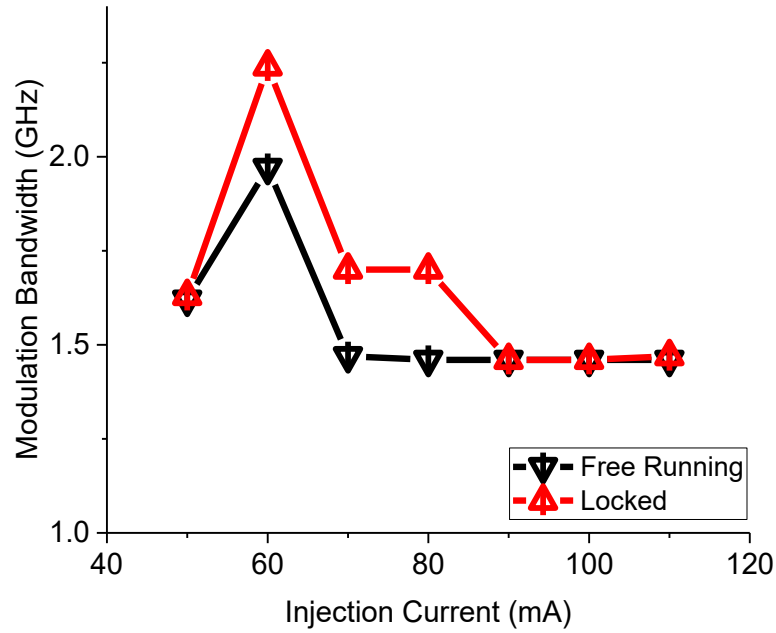


Figure 3-14 Variation of the modulation bandwidth as a function of injection current for red laser diodes.

We further investigated the self-locking characteristics of the BGR laser diodes at different injection currents and at corresponding fixed maximum R values of -1.25 , -3 and -2.22 dB . Figure 3-15, Figure 3-16, and Figure 3-17 compares the spectral linewidths of the self-locked and free running cases at different injection currents above the threshold value. In general, the spectral linewidth is found to decrease noticeably in the locked case and observed to be independent of the injection current, thanks to the injection-locking phenomenon. Considering the blue laser diode, a reduction in the spectral linewidth by > 0.4 nm is measured in the injection current range of $40 - 90$ mA and a maximum value of ~ 0.8 nm, corresponding to ~ 8.3 times improvement, is observed at 80 mA. However, beyond 90 mA a degradation in the improvement factor is observed that is ascribed to the deteriorating laser performance, quantum efficiency in particular, at high injections. On the

other hand, self-locked FP modes of the green laser diode are found to be stable exhibiting an average value of ~ 0.17 nm in the entire range of injection current (40– 160 mA) and with a maximum of 1.11 nm (~ 5 times) improvement was observed at 150 mA. The scope of improvement in red laser diode was found to be less with a measured ~ 0.23 nm spectral linewidth improvement at 110 mA injection current, as illustrated in Figure 3-16. We postulate that a single mode operation (owing to the high-quality active region design and growth) at almost every injection current might be the reason behind this minute enhancement. It is to be noted that the spectral linewidth of the laser diodes is measured at FWHM in both self-locked and free running scenario, owing to the observation of single (multiple) self-locked mode operation at lower (higher) injection currents.

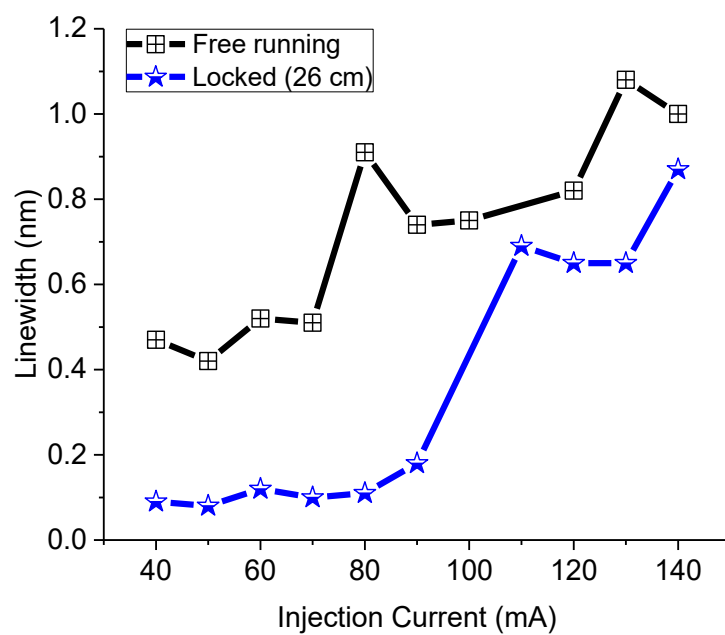


Figure 3-15 Variation of the spectral linewidth as a function of injection current for blue laser diodes.

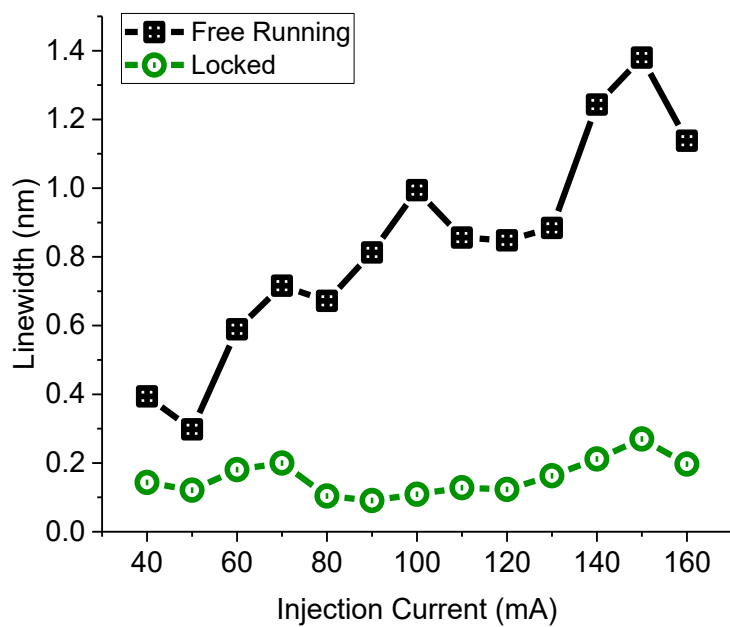


Figure 3-16 Variation of the spectral linewidth as a function of injection current for green laser diodes.

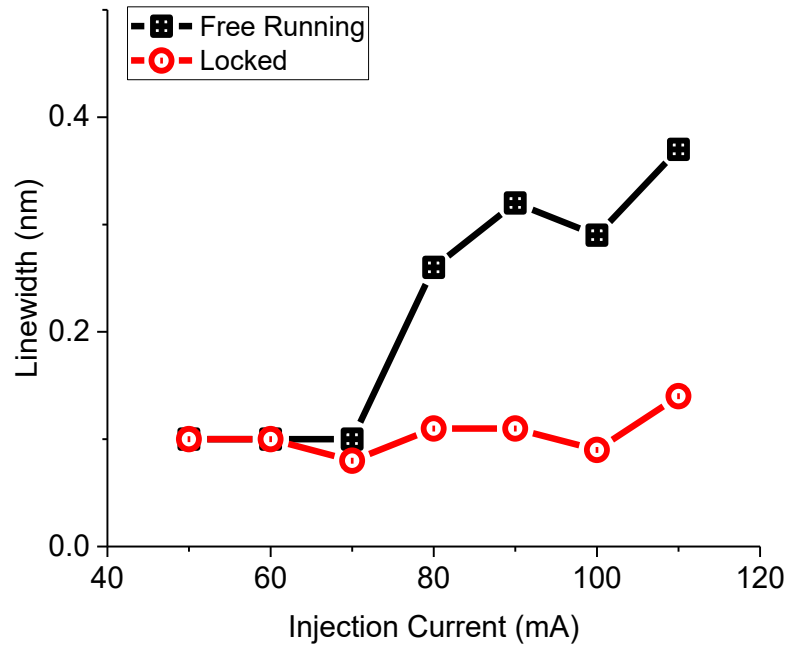


Figure 3-17 Variation of the Spectral linewidth as a function of injection current for red laser diodes.

3.7 Effect of injection ratio on Self-injection locking

The effect of injection ratio on the modulation bandwidth is shown in Figure 3-18, Figure 3-19, and Figure 3-20 for the BGR lasers, respectively. The experiments for blue, green, and red laser diodes were carried out at 70, 120, and 60 mA, respectively. As expected, increasing the injection ratio substantially enhances the modulation bandwidth in all the three color laser diodes under self-injection locking, thanks to the increased feedback power into the laser active region. For the blue and green laser diode, we hypothesize that both these characteristics contributed to the modulation bandwidth improvement. A maximum enhancement by ~880 MHz (1.53 – 2.41 GHz) for green, ~540 MHz (1.72 –

2.26 GHz) for the blue and ~ 320 MHz (1.92 – 2.24 GHz) for the red laser diodes are achieved compared to the free running case.

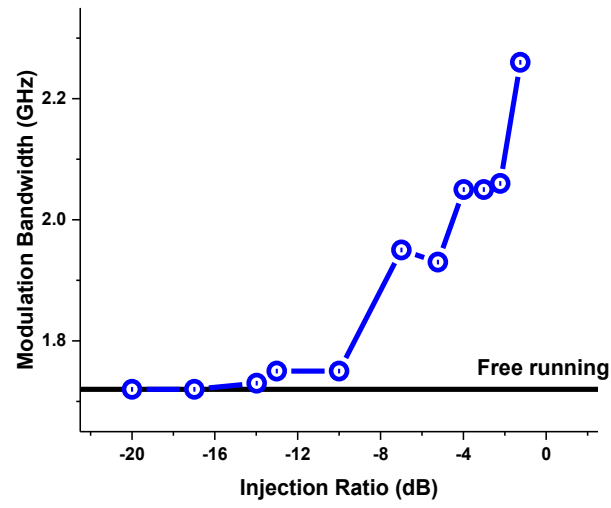


Figure 3-18 Variation of the modulation bandwidth as a function of injection ratio for the blue laser diode.

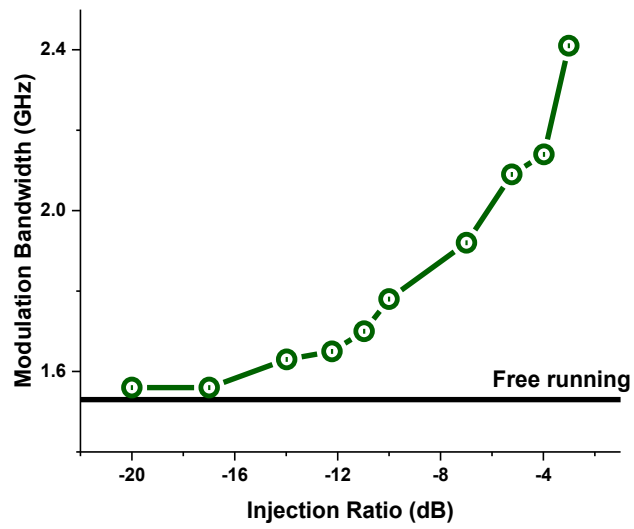


Figure 3-19 Variation of the modulation bandwidth as a function of injection ratio for the green laser diode.

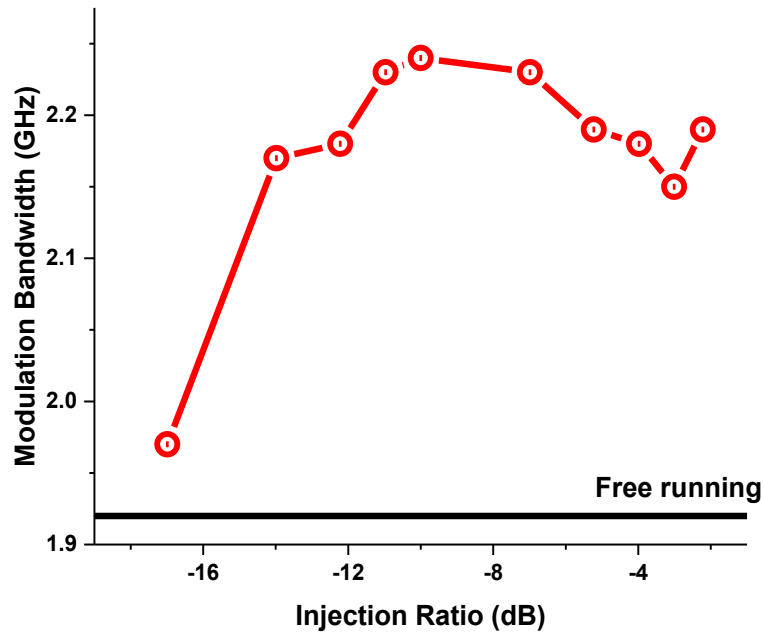


Figure 3-20 Variation of the modulation bandwidth as a function of injection ratio for the red laser diode.

Power injection ratio ' R ' plays a vital role in laser dynamics. It is directly proportional to the spectral linewidth reduction and the mode stability when the round trip phase of the feedback power is zero [17]. It has been shown that bi-stability or multi-stability (*i.e.*, dual or multiple locked modes) might occur with an inverse phase at the optical feedback. To demonstrate the impact of R on the linewidth and modulation bandwidth of the self-injection locked laser diodes, we employed an optical filter to control the feedback power to be re-injected into the laser front facet. The results of blue and green laser diodes, which are illustrated in Figure 3-21 and Figure 3-22, depicts a significant linewidth reduction with increasing injection ratio and later saturates at high injection ratios. Thanks to the increase in the peak power of the locked mode with increasing injection ratio (higher self-feedback power), which dictated this performance improvement. However, this behavior is not

observed in the red laser diode, and an average spectral linewidth of ~ 0.1 nm is measured at all injection ratios attaining the value of the free running case. Note that two different experiments of Figure 3-17 and Figure 3-23 demonstrate a similar measured value of spectral linewidth at fixed $R = -2.22$ dB when the injection current is 60 mA. None of those show any significant improvement in the linewidth, thus further affirming the consistency of our measurements. Moreover, Figure 3-21 and Figure 3-22 exhibited two regimes; one is the linewidth improvement regime up to $R = -12.22$ dB, and saturation regime beyond -12.22 dB, where the linewidth does not improve further. The red laser diode results follow similar trend except there is no improvement in the linewidth in both the regimes. We firmly believe that a proper selection of injection current, perhaps at 80 mA, would enable observation of both the linewidth regimes. A maximum improvement in linewidth by ~ 9 times for blue, ~ 6 times for green, and 1.25 times for red color laser diodes are achieved, which corresponds to ~ 0.07 nm, ~ 0.14 nm and ~ 0.08 nm, at $R = -2.2$ dB, -12.22 dB, and -12.22 dB, respectively.

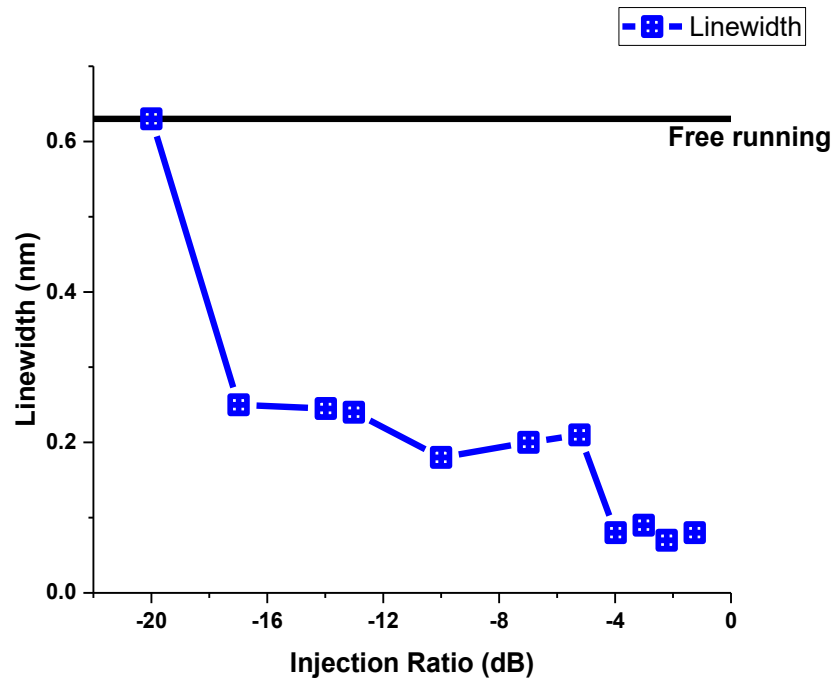


Figure 3-21 Variation of the spectral linewidth as a function of injection ratio for the blue laser diode.

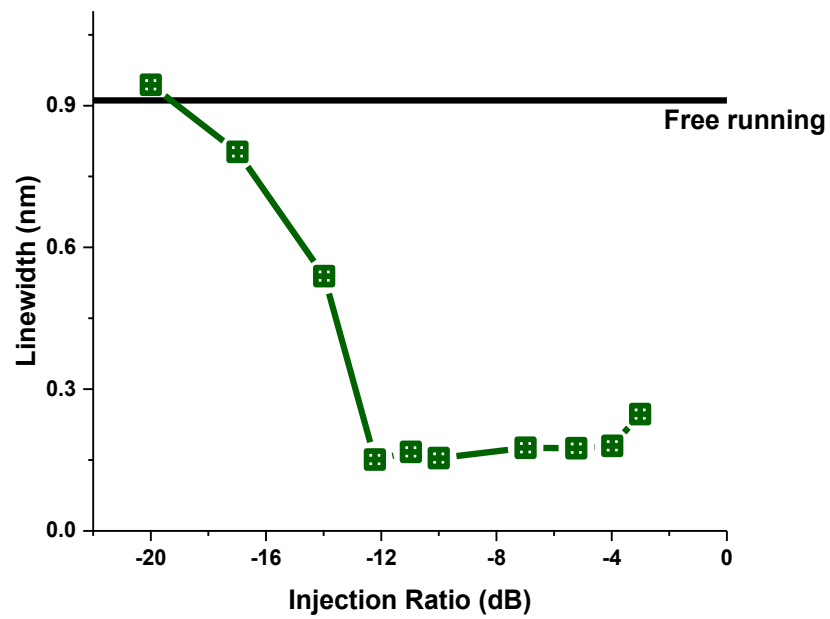


Figure 3-22 Variation of the spectral linewidth as a function of injection ratio for the green laser diode.

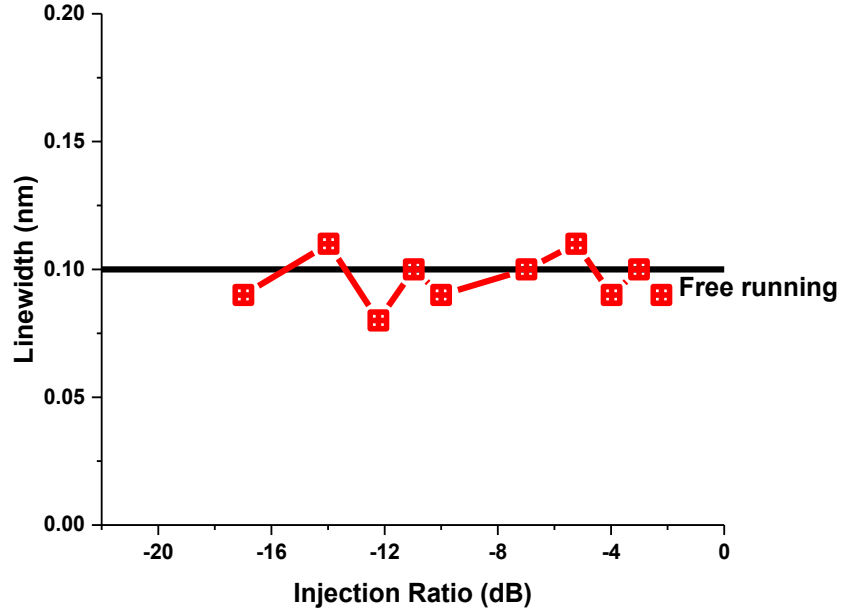


Figure 3-23 Variation of the spectral linewidth as a function of injection ratio for the red laser diode.

3.8 Effect of external cavity length on Self-injection locking

In this section, the effect of external cavity length on the performance of self-injection locked BGR laser diodes is studied. The results of changing L_{ext} from 26 cm to 56 cm on the spectral linewidth and the modulation bandwidth is compared in Figure 3-24 (a) – (c) and (d) – (f), respectively. At higher injection current, the performance of the longer external cavity (56 cm) is found to degrade faster than the shorter cavity and reaches close to the free-running case. For instance, the spectral linewidth of the longer cavity starts to degrade at early injection current of 60 (100) mA compared to the shorter cavity length that showed performance degradation from 80 (120) mA for the blue (green) laser diodes. On the other hand, red laser diode showed performance degradation from a similar current

value of 70 mA from both the cavity lengths. This is attributed to the inferior estimated R value of the longer cavity system due to the additional path and scattering losses compared to the shorter cavity length, and are estimated to be -1.6, -4.0 and -3.0 dB. Hence, a poorer performance from longer cavity is obvious and is in good agreement with the results elucidated in the previous section. As expected, the modulation bandwidth at longer cavity length also exhibited performance degradation in self-injection locked BGR lasers, and attain the finest values as tabulated in Table 3-1. Moreover, the results from 26 cm cavity length are also included alongside for comparison purpose. A maximum improvement of the modulation bandwidth of 240 MHz (1.48 GHz to 1.72GHz) and ~ 4.6 times (0.42 nm to 0.09 nm) reduction in the linewidth for blue, ~ 500 MHz (1.53 GHz to 2.03GHz) and ~ 7.4 times (0.67 nm to 0.09 nm) for green, and 80 MHz (1.47 GHz to 1.55GHz) and ~ 2 times (0.37 nm to 0.18 nm) for red laser diode is measured with the 56 cm cavity length. In general, the performance of self-injection locking in an external cavity is found to be dictated primarily by the variation in the power injection ratio due to the cavity length.

Table 3-1 Performance comparison of 26 and 56 cm external cavity lengths on self-injection locked BGR laser diodes

External cavity length		26 cm		56 cm	
Blue	Injection ratio (dB)	-1.3		-1.6	
	Injection current (mA)	70	80	70	80
	Spectral linewidth (nm)	0.1	0.11	0.4	0.47
	Modulation bandwidth (~GHz)	2.26	2.04	1.93	1.82
Green	Injection ratio (dB)	-3.0		-4.0	
	Injection current (mA)	100	120	100	120
	Spectral linewidth (nm)	0.11	0.12	0.23	0.59
	Modulation bandwidth (GHz)	2.04	2.41	2	2.03
Red	Injection ratio (dB)	-2.2		-3.0	
	Injection current (mA)	60	100	60	100
	Spectral linewidth (nm)	0.09	0.09	0.09	0.15
	Modulation bandwidth (GHz)	2.24	1.53	2	1.53

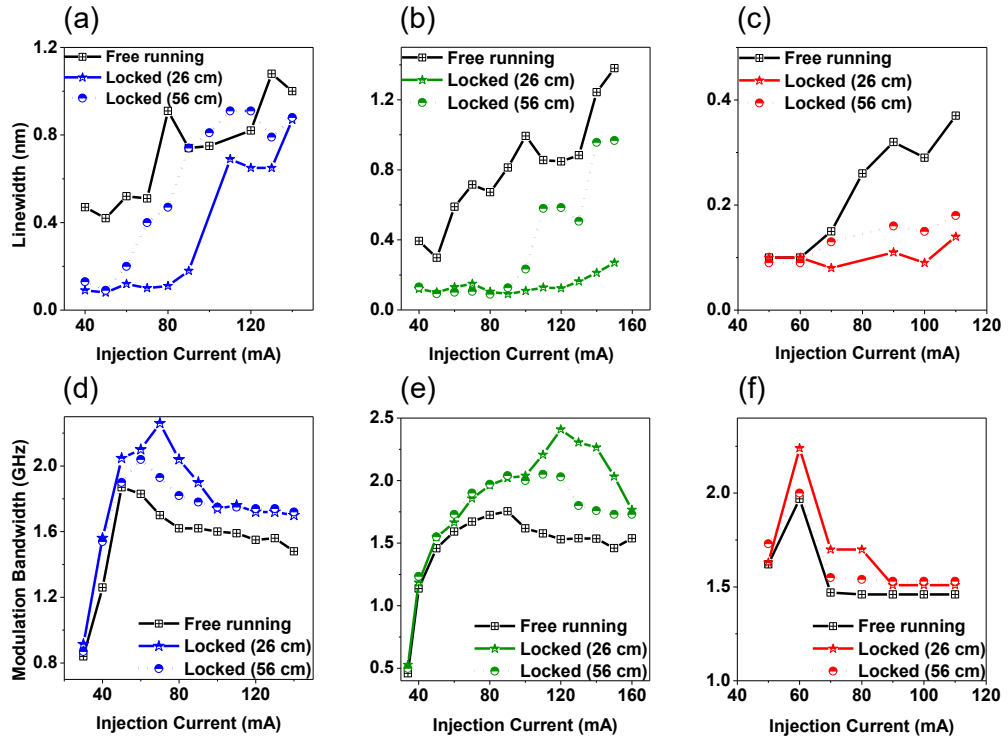


Figure 3-24 Variation of the spectral linewidth (top row) and modulation bandwidth (bottom row) as a function of injection current for blue (a) and (d), green (b) and (e), and red (c) and (f) laser diodes.

CHAPTER 4

VISIBLE LIGHT COMMUNICATION

Very recently, two-stage external injection locking has been introduced by Lin et al. [36] in 680 nm vertical cavity surface emitting lasers (VCSEL) and showed a 56 Gb/s transmission rate using pulse amplitude modulation (PAM4) scheme in a 20 m indoor free space channel. Subsequently, a successful improvement in the modulation bandwidth from 5.2 GHz to 26 GHz and 41.8 GHz using two and three-stage injection locked VCSELs was observed and 25 and 40 Gb/s data rate was demonstrated in a 50 m indoor free space channel [46]. Also, an increase in the peak optical power was observed in their experiment after employing the external injection locking. Lu et al. also explored two-stage injection locking in underwater optical wireless communication using 16-QAM orthogonal frequency division multiplexed (OFDM) modulation scheme at 405 nm violet laser [47]. In that paper, successful transmission of 9.6 Gb/s signal over 8 m underwater link was demonstrated. Moreover, utilization of self-injection locking in communication using visible laser diodes has not been reported yet, to the best of our knowledge. In the subsequent sections of this chapter, the free space communication using a free running laser and self-injection locked laser has been compared. In our experiment, we have used non return to zero on off keying (OOK) modulation scheme.

4.1 On-off keying (OOK)

The non-return to zero (NRZ) signal from the bit error rate tester (BERT, Agilent N4903B J-BERT) was used to modulate the laser diodes. In the receiver side, we have used an avalanche photodetector (APD) or an ultrafast photodetector (UPD) depending on the availability of the devices. As a reflector, we have used a mirror, or a partially reflective polka dot beamsplitter since both of them work as a reflector with different optical feedback.

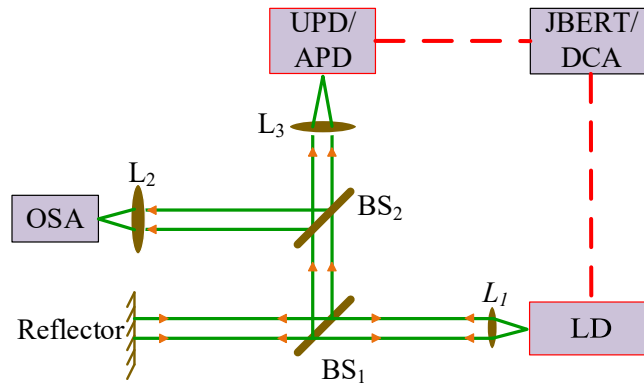


Figure 4-1 Block diagram of On Off Keying (OOK) setup

4.1.1 Effect of the NRZ modulating signal on the SNR:

We have tested the performance of various amplitudes of the modulating NRZ signal from the bit error rate tester (J-BERT) to identify the most suitable operating condition for the communication. The performance curve was measured by plotting SNR as a function of the NRZ signal amplitude and is presented in Figure 4-2. We didn't require to use the TIA since the responsivity of the APD is at least a degree higher than the UPD. Moreover, APD requires smaller amplitude of the modulating signal. It is obvious that the numbers in both

the axes of the following figure will change if UPD was used, while preserving the similar curve.

In the experiment, we have considered 57 mA as the injection current at 20° C temperature. A $2^{10} - 1$ pseudo-random binary sequence (PRBS) was sent in the transmission channel for a data rate of 622 Mbps from the JBERT to measure the signal to noise ratio (SNR). The SNR rises as the modulating signal increases and starts to fall and saturates at a higher amplitude. In this case, it gave the best performance at 140 mV for free running laser, and 160 mV for self-injection locked laser. Similar results were also found for communication with 1.5 Gb/s and 2 Gb/s data rate. One thing to note that the peak SNR shifted to the left of the modulation amplitude as the data rate was increased.

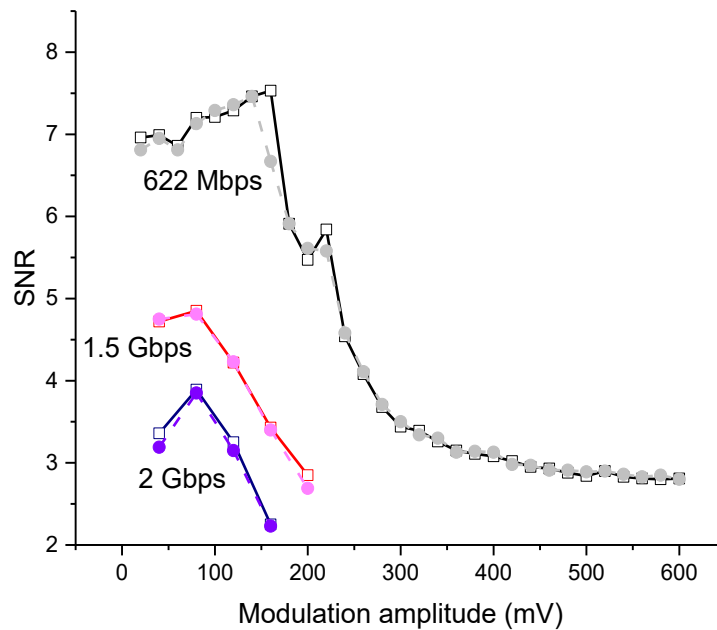


Figure 4-2 Performance of VLC using a 638 nm red LD at various amplitude of the NRZ modulating signal.

4.1.2 Effect of the NRZ modulating signal on the peak wavelengths:

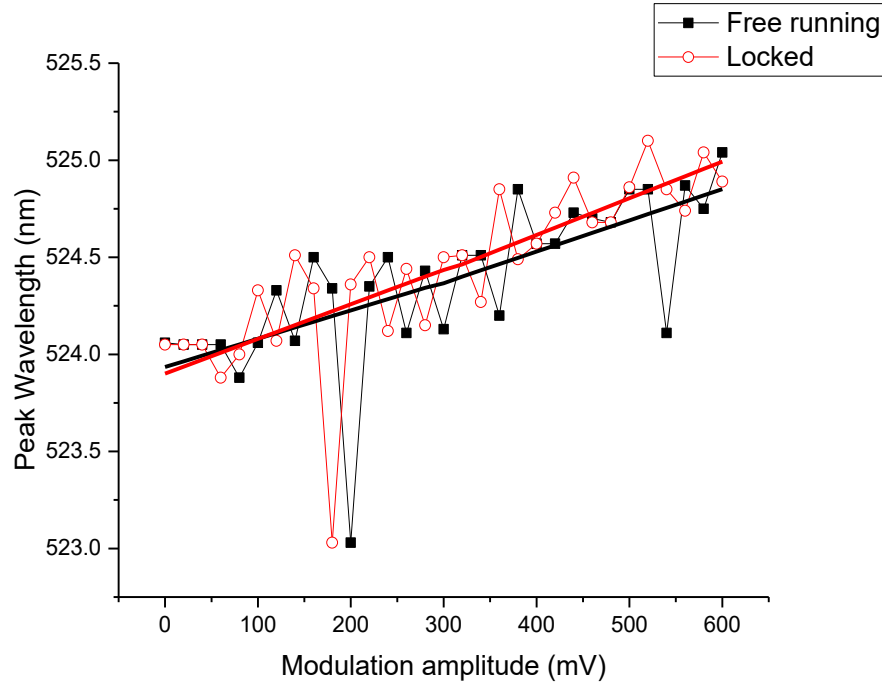


Figure 4-3 Peak wavelength shift of the free running and locked laser at variable amplitude of the modulating signal

While doing the OOK, it was observed that the spectrum shifts to the higher wavelength as the modulating signal increases. From Figure 4-3, we observe that the locked spectrum is leading the free running spectrum by 20 mV, and a pattern emerged which suggest a red shift of the spectrum as we increased the amplitude of the PRBS. The operating parameter is same as it was for Figure 4-2.

4.1.3 Communication using blue laser diode:

Communication using blue laser diode was done at 78 mA injection current and 28.1° C temperature. The corresponding optical spectrum is presented in Figure 4-4. At this

particular point, the right most longitudinal mode is locked. The peak power of the locked mode raised more than twice, accumulating all the power from the other unlocked modes.

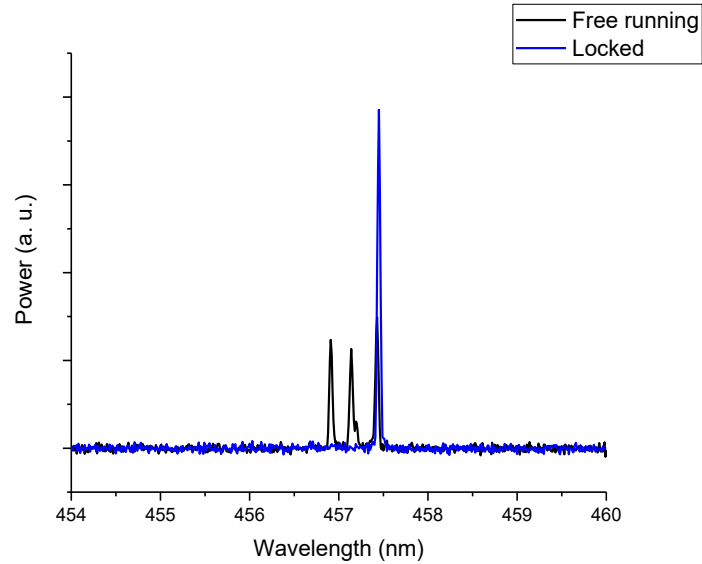
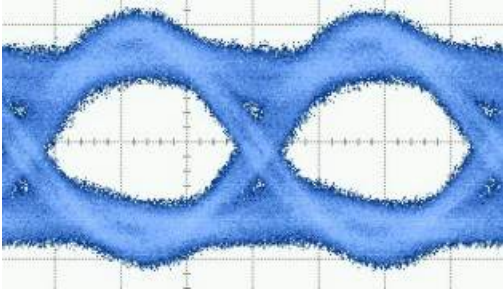
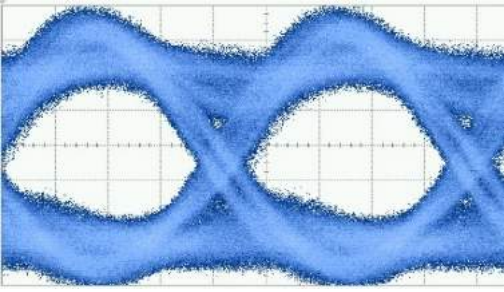
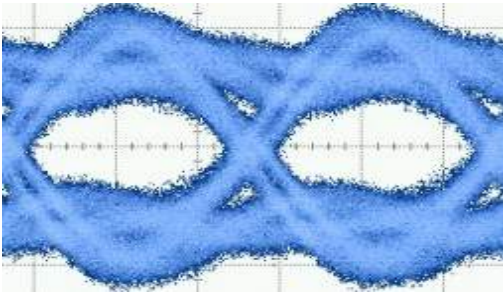
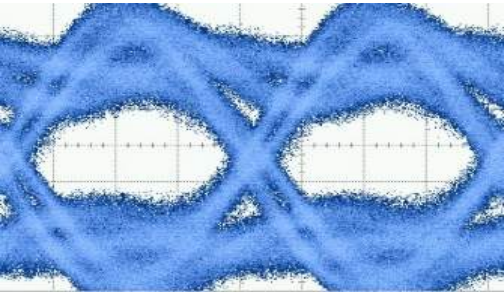
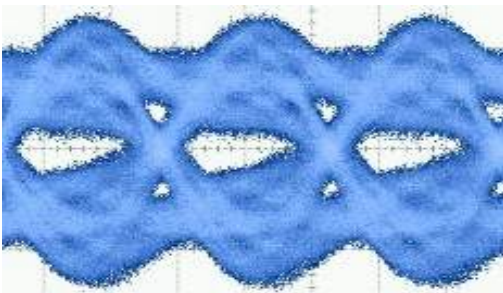
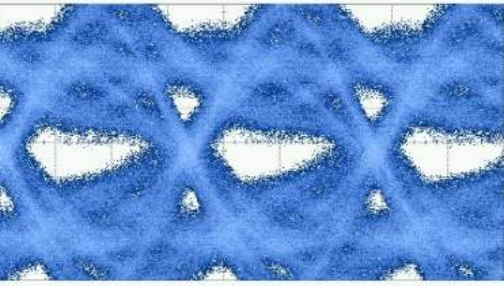
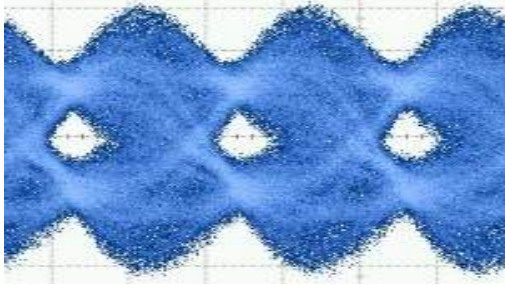
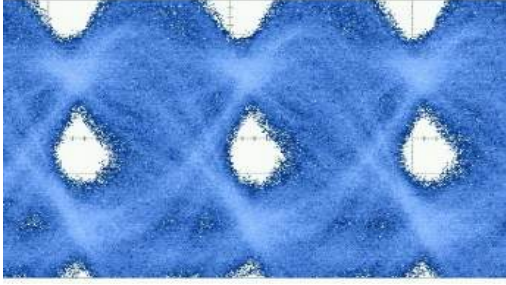
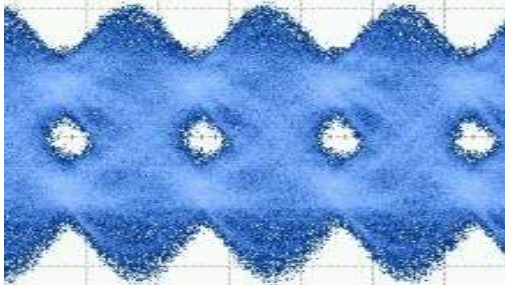
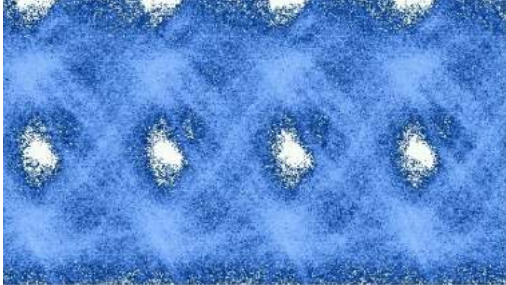


Figure 4-4 Optical spectrum comparing the free running and locked spectrum at 78 mA injection current

Table 4-1 shows the eye test results obtained from the digital communication analyzer (DCA) where the free running and self-injection locked lasers are compared. In all the cases, the free running laser performed better. We can have a clear idea about the communication performance of both the cases from Figure 4-5 Bit error rate of free running (black) and locked (blue) laser at various data rate. where the bit error rate (BER) has been plotted against the data rate. Up to 2 Gbps, the BER of both cases are below the forward error correction (FEC) limit of 3.8×10^{-8} . However, the BER did not reduce due to the self-injection locking as it was expected.

Table 4-1 Eye diagram of the VLC with 450 nm laser diode as a transmitter

Data Rate (Gb/s)	Unlocked	Locked
1		
1.25		
1.5		
1.75		

		
2		

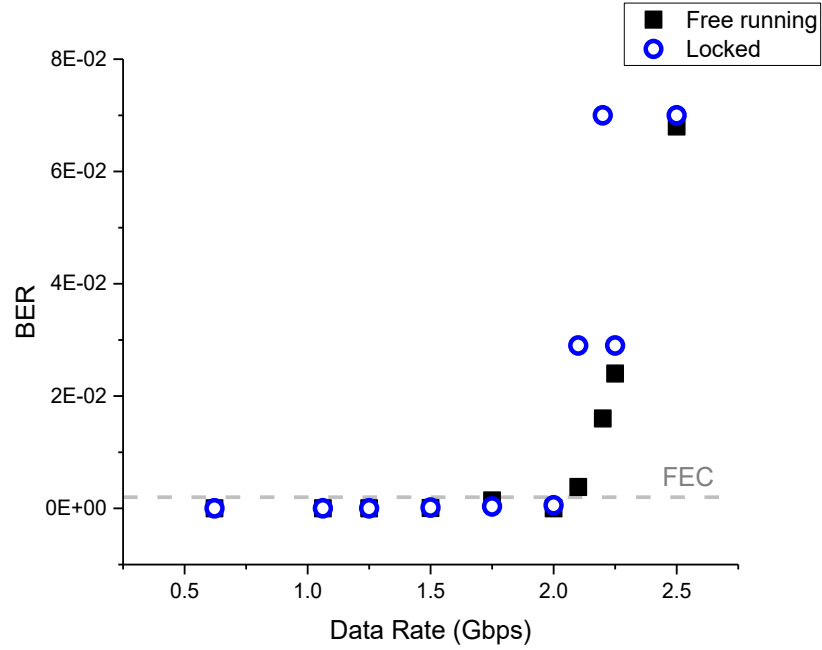


Figure 4-5 Bit error rate of free running (black) and locked (blue) laser at various data rate.

4.1.4 Communication using green laser diode:

Using the Ultrafast Photodiode (UPD-50-UP, Alphalas) as a receiver and the 520 nm green laser diode (L520P50) as a transmitter, we have performed On-Off-Keying (OOK); the laser was operated at 143 mA pumping current and 20°C temperature. The eye diagrams of the transmission results are compared for both locked and free running case in Table 4-2. The corresponding bit error rate (BER) is also plotted in Figure 4-6. Except for 3 Gbps transmission, all of the other data rates are showing degraded performance as we have observed for blue lasers. As a performance parameter, we have considered SNR because of some technical issue with the JBERT. At 3 Gbps the SNR improved from 3.81 to 5.15. The corresponding BER can be found by using equation 4.1

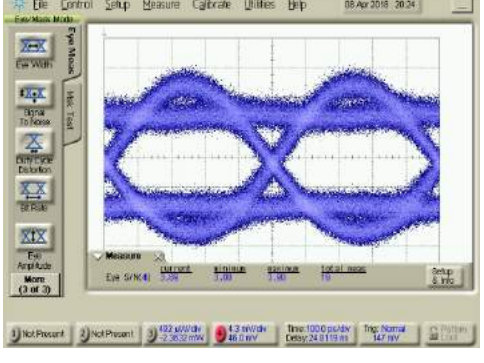
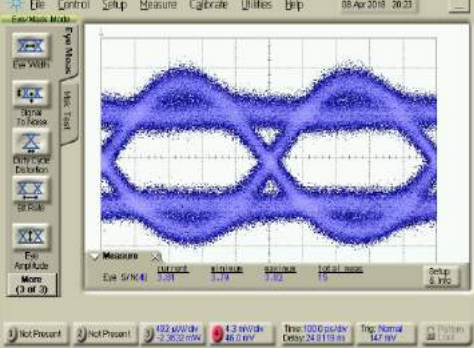
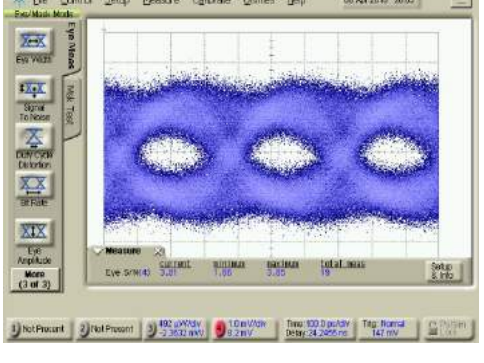
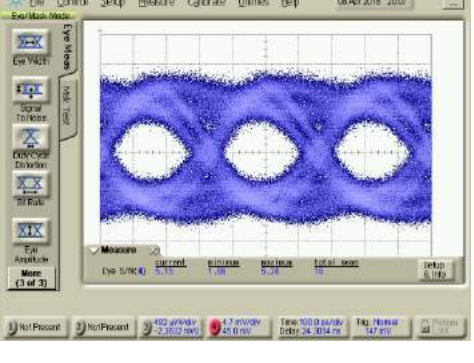
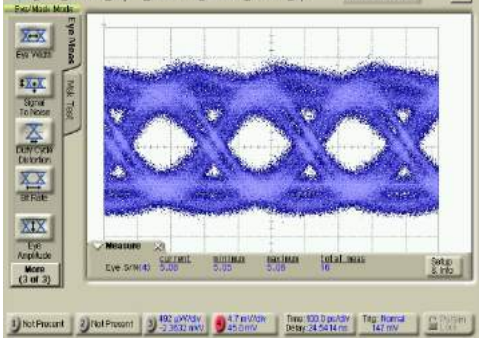
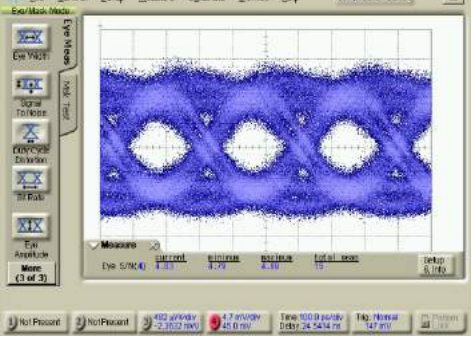
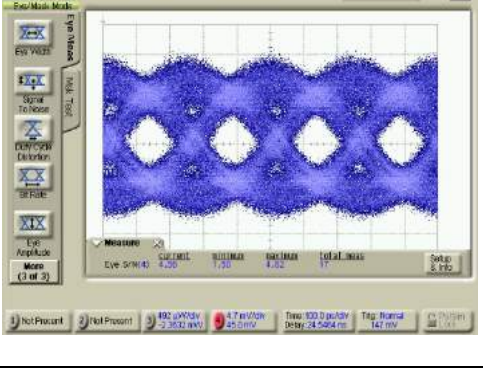
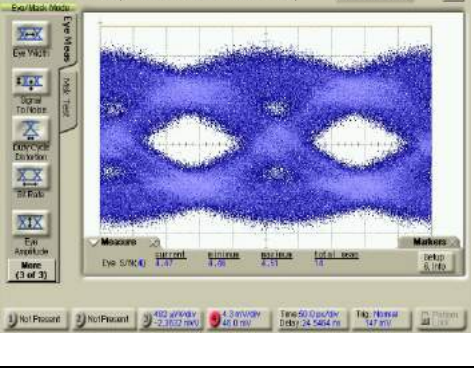
$$BER = \frac{1}{2} \operatorname{erfc}\left(\frac{SNR}{2}\right)$$

4.1

From Figure 4-6, we also observe that the BER at 2-3 Gb/s is worse than 4 Gb/s, which is unlikely to happen. It was because, the operating NRZ amplitude was not varied which is essential to get the best performance at any data rate. The NRZ amplitude is an important factor to consider to get a good, BER and it varies with the data rate as it is shown in Figure 4-2. Finally, up to a 4 Gb/s VLC transmission where the BER is below the FEC limit is shown in Table 4-2.

Table 4-2 Eye diagram for various data rate are compared between free running and locked 520 nm green laser diodes

Bit rate (Gbps)	Free running	Locked
1		
1.5		

2		
3		
3.5		
4		

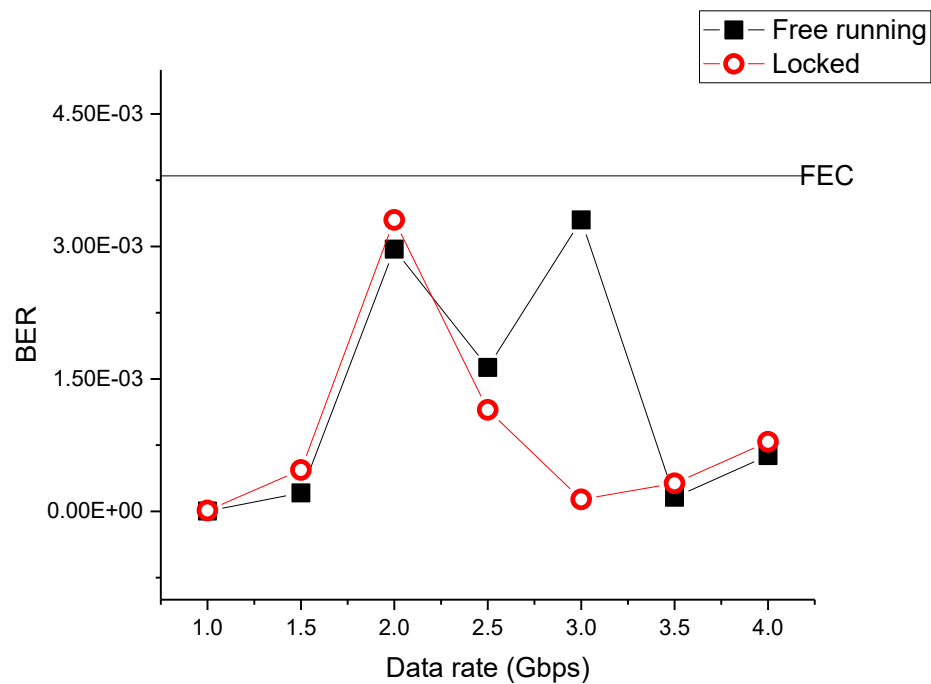
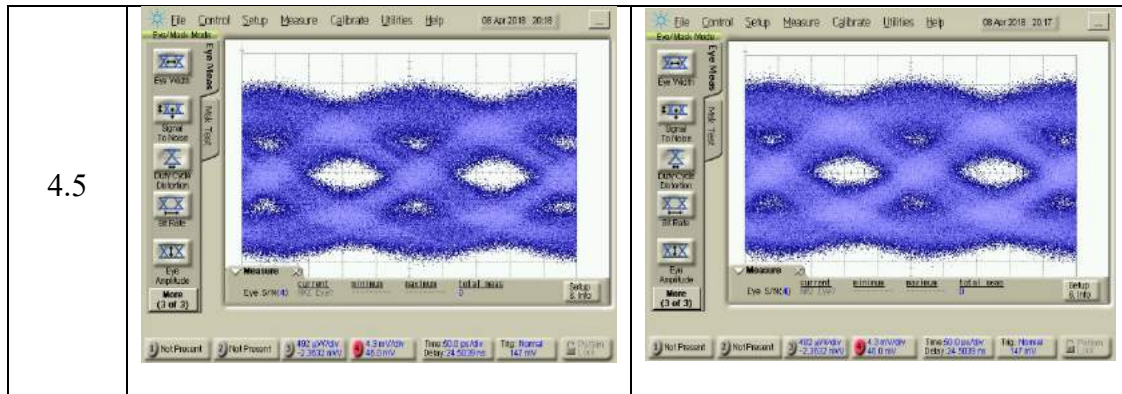


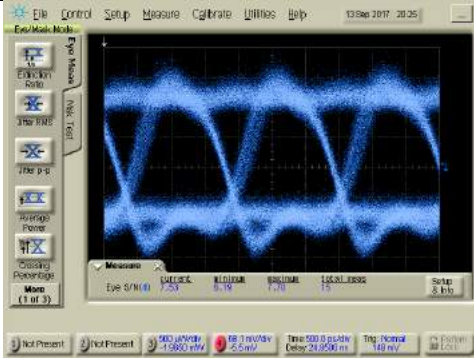
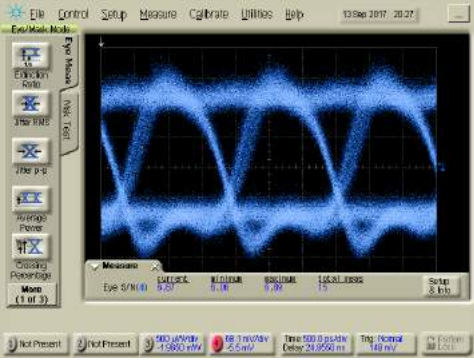
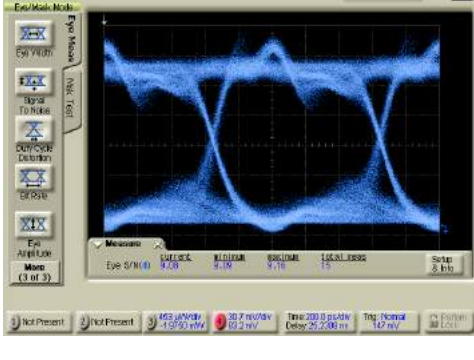
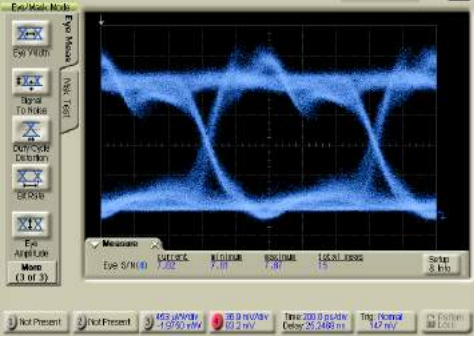
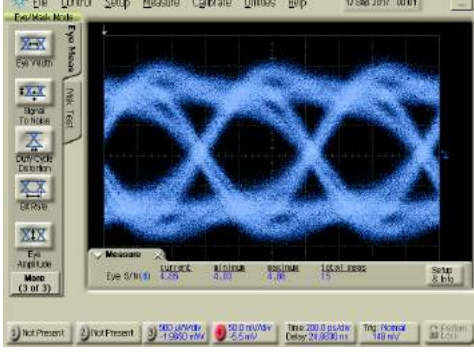
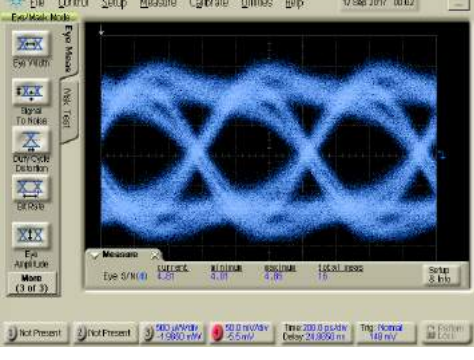
Figure 4-6 Calculated BER for free running and locked 520 nm green laser diode in OOK modulation scheme.

4.1.5 Communication using red laser diode:

638 nm red laser diode also shows the similar degrading performance in self-injection locked case. In this case, we have considered different injection current and NRZ amplitude to get the best performance in both the cases. The eye comparison is shown in Table 4-3, and the corresponding BER, obtained from the SNR, is presented in Figure 4-7. However,

we were successfully able to achieve 2 Gbps VLC which satisfy the FEC limit using the APD as the receiver.

Table 4-3 Eye diagram for various data rate are compared between free running and locked 638 nm red laser diodes

Bitrate (Gbps)	Free running	Locked
0.622		
1		
1.5		

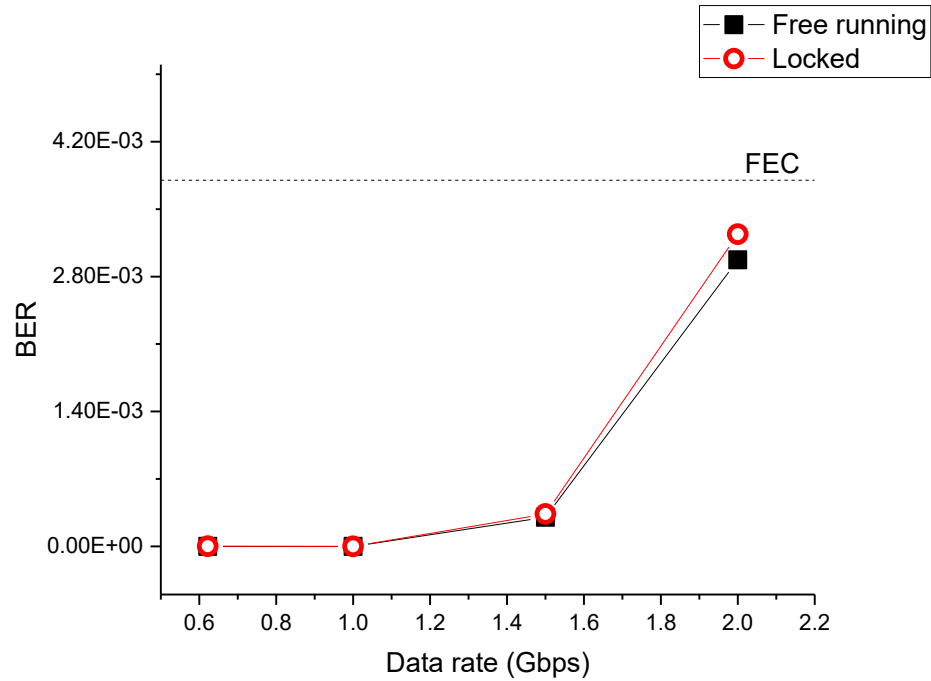
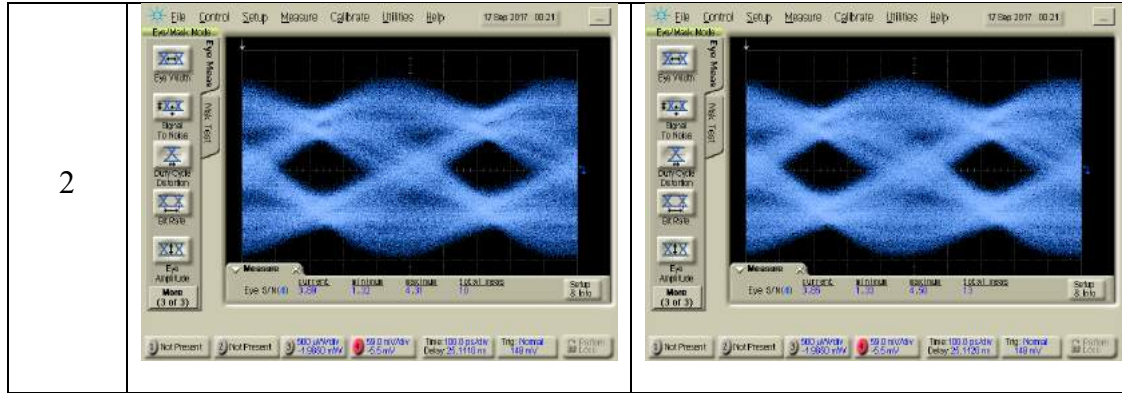


Figure 4-7 Bit error rate (BER) for free running and locked 638 nm red laser diode in OOK modulation scheme.

4.2 Performance analysis of the self-injection locked laser using OOK

From the figures of section 4.1, we have observed that the self-injection locked lasers are not performing better than the free running lasers. We would like to highlight the reasons behind this phenomenon and its possible solution.

a. Formation of peaks and valleys in the frequency response:

As it was shown in Figure 3-8, Figure 3-9, and Figure 3-10 for blue, green, and red lasers respectively, there are peaks and valleys in the frequency response curves. It formed because of the external cavity resonance. The separation between the peaks is inversely proportional to the length of the external cavity as is described in section 3.4. Due to these peaks and valleys, a significant portion of the frequency spectrum becomes unusable. Therefore, enhancement of modulation bandwidth gets nullified. To overcome this problem, the author suggests reducing the external cavity to 1 cm. It requires special consideration in the system. Also, it needs to be mentioned that the stability of the locked laser might be hampered in such small external cavity.

b. Locking phenomenon is hampered by the NRZ signal in OOK:

From Figure 4-3, it can be seen that the peak wavelengths for the locked and free running laser are not the same and it shifts from its position if the amplitude is changed; it gives an impression that the NRZ signal plays an important role in the laser internal dynamics. Being said that, we postulate that the performance of the self-injection locking is significantly hampered by the NRZ signal generated by the JBERT. In this circumstance, we propose to use the external modulator where the linewidth improvement as described in section 3.3 will help greatly. It also will make it possible to incorporate the phase modulation in the system. Due to the limitation of the resources the author could not try this solution.

CHAPTER 5

CONCLUSION

Self-injection locking which is also known as optical feedback or self-seeded locking is a popular topic since a long time. The advent of mode-locked laser, which is made with the help of an external cavity, came as a solution for high speed data connectivity in the current world. However, this kind of laser is not available in the visible wavelength. The demand for high data rate transmission cannot be realized without a mode-locked laser. In our work, we have demonstrated the proof of concept that with the current GaN laser, it is possible to make a mode-locked laser.

5.1 Summary of the research contribution

We have achieved 1.5 times improvement in the modulation bandwidth and 10 times reduction in the linewidth. SMSR has also improved significantly. All these parameters are essential to have a high-speed communication.

We have demonstrated the communication using On Off Keying (OOK) scheme in both free running and injection locked laser. We were able to show a maximum of 4 Gbps data transmission rate, which was limited by the bandwidth of the photodetector.

5.2 Future work

From the results and experience from this work, we recommend the following work to be done in future.

- A mode-locked laser can be fabricated where the external cavity would be very small, 1 cm to ensure a frequency response which is free from the peaks and valleys. A high data rate communication would be possible with a compact ECDL system.
- An external modulator can be used for the transmission experiment. The narrow linewidth should help in achieving high data rate communication. Unfortunately, a high speed external modulator is still not available in the market. Phase modulation may also be performed using an external modulator.

References

- [1] Wikipedia, “Lighthouse.” [Online]. Available: <https://en.wikipedia.org/wiki/Lighthouse>.
- [2] Wikipedia, “Wireless.” [Online]. Available: <https://en.wikipedia.org/wiki/Wireless#Photophone>.
- [3] J. C. Maxwell, “A treatise on electricity and magnetism,” *Oxford Clarendon Press*, vol. 1, 1881.
- [4] Wikipedia, “Jagadish Chandra Bose.” [Online]. Available: https://en.wikipedia.org/wiki/Jagadish_Chandra_Bose.
- [5] A. L. Schawlow and C. H. Townes, “Infrared and Optical Masers,” *Phys. Rev.*, vol. 112, no. 6, pp. 1940–1949, Dec. 1958.
- [6] K. C. Kao and G. A. Hockham, “Dielectric-fibre surface waveguides for optical frequencies,” *Proc. Inst. Electr. Eng.*, vol. 113, no. 7, pp. 1151–1158, Jul. 1966.
- [7] “Cisco Visual Networking Index: Forecast and Methodology, 2016-2021,” 2017.
- [8] Wikipedia, “Visible spectrum.” [Online]. Available: https://en.wikipedia.org/wiki/Visible_spectrum#/media/File:Linear_visible_spectrum.svg.
- [9] J. Wang, M. K. Haldar, L. Li, and F. V. C. Mendis, “Enhancement of modulation bandwidth of laser diodes by injection locking,” *IEEE Photonics Technol. Lett.*, vol. 8, no. 1, pp. 34–36, Jan. 1996.
- [10] O. I. Permyakova, A. V. Yakovlev, and P. L. Chapovsky, “Simple external cavity diode laser,” Dec. 2003.
- [11] K. C. Harvey and C. J. Myatt, “External-cavity diode laser using a grazing-incidence diffraction grating,” *Opt. Lett.*, vol. 16, no. 12, p. 910, Jun. 1991.
- [12] Thorlabs, “L450B,” 2013. [Online]. Available: <https://www.thorlabs.com/drawings/f4b26f0bbb073cf0-1D63605C-A03D-CDAA-6BD56F6652038243/PL450B-MFGSpec.pdf>.
- [13] Thorlabs, “L520P50,” 2015. [Online]. Available: <https://www.thorlabs.com/drawings/f4b26f0bbb073cf0-1D63605C-A03D-CDAA-6BD56F6652038243/L520P50-SpecSheet.pdf>.
- [14] Thorlabs, “L638P040,” 2017. [Online]. Available: <https://www.thorlabs.com/drawings/f4b26f0bbb073cf0-1D63605C-A03D-CDAA-6BD56F6652038243/L638P040-SpecSheet.pdf>.

- [15] J. Mørk, B. Tromborg, and J. Mark, "Chaos in semiconductor lasers with optical feedback: theory and experiment," *IEEE J. Quantum Electron.*, vol. 28, no. 1, pp. 93–108, 1992.
- [16] Y. SHEVY, J. KITCHING, and A. YARIV, "Linewidth Reduction and Frequency Stabilization of a Semiconductor-Laser With a Combination of Fm Side-Band Locking and Optical Feedback," *Opt. Lett.*, vol. 18, no. 13, pp. 1071–1073, 1993.
- [17] K. Petermann, "External optical feedback phenomena in semiconductor lasers - Selected Topics in Quantum Electronics, IEEE Journal on," *IEEE J. Quantum Electron.*, vol. 1, no. 2, pp. 480–489, 1995.
- [18] A. Zadok, H. Shalom, M. Tur, W. D. Cornwell, and I. Andonovic, "Spectral shift and broadening of DFB lasers under direct modulation," *IEEE Photonics Technol. Lett.*, vol. 10, no. 12, pp. 1709–1711, 1998.
- [19] S. Sivaprakasam, E. Shahverdiev, P. Spencer, and K. Shore, "Experimental Demonstration of Anticipating Synchronization in Chaotic Semiconductor Lasers with Optical Feedback," *Phys. Rev. Lett.*, vol. 87, no. 15, p. 154101, 2001.
- [20] T. Heil, I. Fischer, W. Elsässer, and A. Gavrielides, "Dynamics of Semiconductor Lasers Subject to Delayed Optical Feedback: The Short Cavity Regime," *Phys. Rev. Lett.*, vol. 87, no. 24, p. 243901, 2001.
- [21] T. Heil, I. Fischer, W. Elsässer, B. Krauskopf, K. Green, and A. Gavrielides, "Delay dynamics of semiconductor lasers with short external cavities: Bifurcation scenarios and mechanisms," *Phys. Rev. E*, vol. 67, no. 6, p. 066214, 2003.
- [22] L. Chrostowski, X. Zhao, C. J. Chang-Hasnain, R. Shau, M. Ortsiefer, and M. C. Amann, "50-GHz optically injection-locked 1.55- μ m VCSELs," *IEEE Photonics Technol. Lett.*, vol. 18, no. 2, pp. 367–369, 2006.
- [23] M. Radziunas *et al.*, "Improving the modulation bandwidth in semiconductor lasers by passive feedback," *IEEE J. Sel. Top. Quantum Electron.*, vol. 13, no. 1, pp. 136–142, 2007.
- [24] J. Zamora-Munt, C. Masoller, and J. García-Ojalvo, "Transient low-frequency fluctuations in semiconductor lasers with optical feedback," *Phys. Rev. A - At. Mol. Opt. Phys.*, vol. 81, no. 3, 2010.
- [25] M. Haji *et al.*, "Ultralow 192 Hz RF linewidth optoelectronic oscillator based on the optical feedback of mode-locked laser diodes," *Cleo Si*, vol. 20, no. 3, pp. 3268–74, 2012.
- [26] F. Grillot, C. Wang, N. A. Naderi, and J. Even, "Modulation properties of self-injected quantum-dot semiconductor diode lasers," *IEEE J. Sel. Top. Quantum Electron.*, vol. 19, no. 4, 2013.
- [27] M. Ahmed, A. Bakry, R. Altuwirqi, M. S. Alghamdi, and F. Koyama, "Enhancing modulation bandwidth of semiconductor lasers beyond 50 GHz by strong optical

- feedback for use in millimeter-wave radio over fiber links,” *Jpn. J. Appl. Phys.*, vol. 52, no. 12, 2013.
- [28] L. Jaurigue, O. Nikiforov, E. Schöll, S. Breuer, and K. Lüdge, “Dynamics of a passively mode-locked semiconductor laser subject to dual-cavity optical feedback,” *Phys. Rev. E*, vol. 93, no. 2, pp. 1–12, 2016.
 - [29] C. Otto, “Dynamics of quantum dot lasers subject to optical feedback and external optical injection.”
 - [30] C. Wang, “Modulation Dynamics of InP- Based Nanostructure Laser and Quantum Cascade Laser,” 2015.
 - [31] R. Lang and K. Kobayashi, “External Optical Feedback Effects on Semiconductor Injection Laser Properties,” *IEEE J. Quantum Electron.*, vol. 16, no. 3, pp. 347–355, 1980.
 - [32] M. T. A. Khan *et al.*, “4 m/100 Gb/s Optical Wireless Communication Based on Far L-Band Injection Locked Quantum-Dash Laser,” *IEEE Photonics J.*, vol. 9, no. 2, pp. 1–7, Apr. 2017.
 - [33] M. Khan, E. Alkhazraji, and A. Ragheb, “100 Gb/s Single Channel Transmission Using Injection-Locked 1621 nm Quantum-Dash Laser,” *IEEE Photonics*, 2017.
 - [34] C.-L. Ying, H.-H. Lu, C.-Y. Li, C.-J. Cheng, P.-C. Peng, and W.-J. Ho, “20-Gbps optical LiFi transport system,” *Opt. Lett.*, vol. 40, no. 14, pp. 3276–9, 2015.
 - [35] C.-Y. Li *et al.*, “16 Gb/s PAM4 UWOC system based on 488-nm LD with light injection and optoelectronic feedback techniques,” *Opt. Express*, vol. 25, no. 10, p. 11598, 2017.
 - [36] X.-Y. Lin *et al.*, “A 56-Gbps PAM4 LiFi Transmission System Based on VCSEL with Two-Stage Injection-Locked Technique,” in *Optical Fiber Communication Conference*, 2017, p. W2A.37.
 - [37] H.-H. Lu *et al.*, “45 Gb/s PAM4 transmission based on VCSEL with light injection and optoelectronic feedback techniques,” *Opt. Lett.*, vol. 41, no. 21, p. 5023, 2016.
 - [38] W. Liang *et al.*, “Ultralow noise miniature external cavity semiconductor laser,” *Nat. Commun.*, vol. 6, 2015.
 - [39] D. . . Kane and K. A. Shore, “Unlocking Dynamical Diversity: Optical Feedback Effects on Semiconductor Lasers,” vol. 1, p. 356, 2005.
 - [40] K. Petermann, “External Optical Feedback Phenomena in Semiconductor Lasers,” *IEEE J. Sel. Top. Quantum Electron.*, vol. 1, no. 2, pp. 480–489, 1995.
 - [41] H. Lu, C. Li, H. Lin, W. Tsai, and C. Chu, “An 8 m/9.6 Gbps Underwater Wireless Optical Communication System,” *IEEE Photonics*, 2016.

- [42] P. L. Christiansen, “Bistability and Low-Frequency Fluctuations in Semiconductor Lasers with Optical Feedback : A Theoretical Analysis,” vol. 24, no. 2, pp. 123–133, 1988.
- [43] T. Heil, I. Fischer, and W. Elsa, “Coexistence of low-frequency fluctuations and stable emission on a single high-gain mode in semiconductor lasers with external optical feedback,” vol. 58, no. 4, pp. 2672–2675, 1998.
- [44] M. Chi, O. B. Jensen, and P. M. Petersen, “Tuning range and output power optimization of an external-cavity GaN diode laser at 455 nm,” *Appl. Opt.*, vol. 55, no. 9, p. 2263, 2016.
- [45] S. Watson *et al.*, “High speed visible light communication using blue GaN laser diodes,” vol. 9991, p. 99910A, 2016.
- [46] W.-S. Tsai *et al.*, “A 50 m/40 Gbps 680-nm VCSEL-based FSO communication,” in *2016 IEEE Photonics Conference (IPC)*, 2016, pp. 39–40.
- [47] H. H. Lu *et al.*, “An 8 m/9.6 Gbps underwater wireless optical communication system,” *IEEE Photonics J.*, vol. 8, no. 5, 2016.

Vitae

Name :Md Hosne Mobarok Shamim
Nationality :Bangladeshi
Date of Birth :10/10/1990
Email :hosnemobarok.shamim@gmail.com
Address :Ka 197/3, Namapara Road, Khilket, Dhaka – 1229,
Bangladesh
Academic Background :M.Sc. in Electrical Engineering,
King Fahd University of Petroleum & Minerals (KFUPM),
Dhahran-31261, Saudi Arabia
B. Sc. in Electrical and Electronic Engineering
Islamic University of Technology (IUT),
Gazipur, Bangladesh

Publications:

Journals:

[J1] **M. Hosne M. Shamim**, M. A. Shemis, C. Shen, H. M. Oubei, T.K. Ng, B. S. Ooi, and M. Z. M. Khan, "Investigation of Self-injection Locked Visible Laser Diodes for High Bit-rate Visible Light Communication", IEEE Photonics Journal, 2018.

<https://doi.org/10.1109/JPHOT.2018.2849884>

Conferences:

[C2] **M. Hosne. M. Shamim**, M. A. Shemis, C. Shen, H. M. Oubei, T. K. Ng, B. S. Ooi, and M. Z. M. Khan, "Enhanced performance of 450 nm GaN laser diodes with an optical feedback for high bit-rate visible light communication," in Conference on Lasers and Electro-Optics, OSA Technical Digest (online) (Optical Society of America, 2018), paper JT2A.29.

https://doi.org/10.1364/CLEO_AT.2018.JT2A.29

[C1] **M. Hosne M. Shamim**, M. A. shemis, C. Shen, H. Oubei, T. Ng, B. Ooi, and M. Khan, "High Performance self-injection locked 524 nm green laser diode for high bitrate visible light communications," in Optical Fiber Communication Conference, OSA Technical Digest (online) (Optical Society of America, 2018), paper Th2A.15.

<https://doi.org/10.1364/OFC.2018.Th2A.15>